

VIRGOS: Secure Graph Convolutional Network on Vertically Split Data from Sparse Matrix Decomposition

Yu Zheng*
yu.zheng@uci.edu
University of California, Irvine

Qizhi Zhang*
zqz.math@gmail.com
Morse Team, Ant Group

Lichun Li
lichun.llc@antgroup.com
Morse Team, Ant Group

Kai Zhou
kaizhou@polyu.edu.hk
Hong Kong Polytechnic University

Shan Yin
yinshan.ys@antgroup.com
Morse Team, Ant Group

Abstract

Securely computing graph convolutional networks (GCNs) is critical for applying their analytical capabilities to privacy-sensitive data like social/credit networks. Multiplying a sparse yet large adjacency matrix of a graph in GCN—a core operation in training/inference—poses a performance bottleneck in secure GCNs. Consider a GCN with $|\mathcal{V}|$ nodes and $|\mathcal{E}|$ edges; it incurs a large $O(|\mathcal{V}|^2)$ communication overhead.

Modeling bipartite graphs and leveraging the monotonicity of non-zero entry locations, we propose a co-design harmonizing secure multi-party computation (MPC) with matrix sparsity. Our sparse matrix decomposition transforms an arbitrary sparse matrix into a product of structured matrices. Specialized MPC protocols for oblivious permutation and selection multiplication are then tailored, enabling our secure sparse matrix multiplication ((SM)²) protocol, optimized for secure multiplication of these structured matrices. Together, these techniques take $O(|\mathcal{E}|)$ communication in constant rounds. Supported by (SM)², we present VIRGOS¹, a secure 2-party framework that is communication-efficient and memory-friendly on standard vertically-partitioned graph datasets. Performance of VIRGOS has been empirically validated across diverse network conditions.

CCS Concepts

• Security and privacy → Cryptography; • Computing methodologies → Machine learning.

Keywords

Secure Sparse Matrix Computation, Secure Graph Learning, Secure Multiparty Computation.

*Yu and Qizhi share the co-first authorship.

¹Vertically-split Inference & Reasoning on GCNs Optimized by Sparsity.

Permission to make digital or hard copies of all or part of this work for personal or classroom use is granted without fee provided that copies are not made or distributed for profit or commercial advantage and that copies bear this notice and the full citation on the first page. Copyrights for components of this work owned by others than the author(s) must be honored. Abstracting with credit is permitted. To copy otherwise, or republish, to post on servers or to redistribute to lists, requires prior specific permission and/or a fee. Request permissions from permissions@acm.org.

Conference acronym 'XX, Woodstock, NY

© 2025 Copyright held by the owner/author(s). Publication rights licensed to ACM.

ACM ISBN 978-1-4503-XXXX-X/18/06

<https://doi.org/XXXXXXXX.XXXXXXX>

ACM Reference Format:

Yu Zheng, Qizhi Zhang, Lichun Li, Kai Zhou, and Shan Yin. 2025. VIRGOS: Secure Graph Convolutional Network on Vertically Split Data from Sparse Matrix Decomposition. In *Proceedings of Make sure to enter the correct conference title from your rights confirmation email (Conference acronym 'XX)*. ACM, New York, NY, USA, 19 pages. <https://doi.org/XXXXXXXX.XXXXXXX>

1 Introduction

Graphs, representing structural data and topology, are widely used across various domains, such as social networks and merchandising transactions. Graph convolutional networks (GCN) [31] have significantly enhanced model training on these interconnected nodes. However, these graphs often contain sensitive information that should not be leaked to untrusted parties. For example, companies may analyze sensitive demographic and behavioral data about users for applications ranging from targeted advertising to personalized medicine. Given the data-centric nature and analytical power of GCN training, addressing these privacy concerns is imperative.

Secure multi-party computation (MPC) [13, 15, 17] is a critical tool for privacy-preserving machine learning, enabling mutually distrustful parties to collaboratively train models with privacy protection over inputs and (intermediate) computations. While research advances (e.g., [21, 29, 37, 41, 46, 51, 56]) support secure training on convolutional neural networks (CNNs) efficiently, private GCN training with MPC over graphs remains challenging.

Graph convolutional layers in GCNs involve multiplications with a (normalized) adjacency matrix containing $|\mathcal{E}|$ non-zero values in a $|\mathcal{V}| \times |\mathcal{V}|$ matrix for a graph with $|\mathcal{V}|$ nodes and $|\mathcal{E}|$ edges. The graphs are typically sparse but large. One could use the standard Beaver-triple-based protocol to securely perform these sparse matrix multiplications by treating graph convolution as ordinary dense matrix multiplication. However, this approach incurs $O(|\mathcal{V}|^2)$ communication and memory costs due to computations on irrelevant nodes. Integrating existing cryptographic advances, the initial effort of SecGNN [45, 55] requires heavy communication or computational overhead. Recently, CoGNN [63] optimizes the overhead in terms of horizontal data partitioning, proposing a semi-honest secure framework. Research for secure GCN over vertical data remains nascent.

Current MPC studies, for GCN or not, have primarily targeted settings where participants own different data samples, *i.e.*, horizontally partitioned data [63]. MPC specialized for scenarios where parties hold different types of features [11, 35, 54] is rare. This paper studies 2-party secure GCN training for these vertical partition

cases, where one party holds private graph topology (e.g., edges) while the other owns private node features. For instance, LinkedIn holds private social relationships between users, while banks own users' private bank statements. Such real-world graph structures underpin the relevance of our focus. To our knowledge, no prior work tackles secure GCN training in this context, which is crucial for cross-silo collaboration.

To realize secure GCN over vertically split data, we tailor MPC protocols for sparse graph convolution, which fundamentally involves sparse (adjacency) matrix multiplication. Recent studies have begun exploring MPC protocols for sparse matrix multiplication (SMM). ROOM [48], a seminal work on SMM, requires foreknowledge of sparsity types: whether the input matrices are row-sparse or column-sparse. Unfortunately, GCN typically trains on graphs with arbitrary sparsity, where nodes have varying degrees and no specific sparsity constraints. Moreover, the adjacency matrix in GCN often contains a self-loop operation represented by adding the identity matrix, which is neither row- nor column-sparse. Araki *et al.* [1] avoid this limitation in their scalable, secure graph analysis work, yet it does not cover vertical partition.

To bridge this gap, we propose a secure sparse matrix multiplication protocol, (SM)², achieving *accurate, efficient, and secure GCN training over vertical data* for the first time.

1.1 New Techniques for Sparse Matrices

The cost of evaluating a GCN layer is dominated by SMM in the form of AX , where A is a sparse adjacency matrix of a (directed) graph \mathcal{G} and X is a dense matrix of node features. For unrelated nodes, which often constitute a substantial portion, the element-wise products $0 \cdot x$ are always zero. Our efficient MPC design avoids unnecessary secure computation over unrelated nodes by focusing on computing non-zero results while concealing the sparse topology. We achieve this by: 1) decomposing the sparse matrix A into a product of matrices (§4), including permutation and binary diagonal matrices, that can *faithfully* represent the original graph topology; 2) devising specialized protocols (§5) for efficiently multiplying the structured matrices while hiding sparsity topology.

1.1.1 Sparse Matrix Decomposition. We decompose adjacency matrix A of \mathcal{G} into two bipartite graphs: one represented by sparse matrix A_{out} , linking the out-degree nodes to edges, the other by sparse matrix A_{in} , linking edges to in-degree nodes.

We then permute the columns of A_{out} and the rows of A_{in} so that the permuted matrices A'_{out} and A'_{in} have non-zero positions with *monotonically non-decreasing* row and column indices. A permutation σ is used to preserve the edge topology, leading to an initial decomposition of $A = A'_{\text{out}} \sigma A'_{\text{in}}$. This is further refined into a sequence of *linear transformations*, which can be efficiently computed by our MPC protocols for *oblivious permutation* and *oblivious selection-multiplication*. Our decomposition approach is not limited to GCNs but also general SMM by treating them as adjacency matrices.

1.1.2 New Protocols for Linear Transformations. *Oblivious permutation* (OP) is a two-party protocol taking a private permutation σ and a private vector X from the two parties, respectively, and

generating a secret share $\langle \sigma X \rangle$ between them. Our OP protocol employs correlated randomnesses generated in an input-independent offline phase to mask σ and X for secure computations on intermediate results, requiring only 1 round in the online phase (*cf.*, ≥ 2 in previous works [1, 2]).

Another crucial two-party protocol in our work is *oblivious selection-multiplication* (OSM). It takes a private bit s from a party and secret share $\langle x \rangle$ of an arithmetic number x owned by the two parties as input and generates secret share $\langle sx \rangle$. Our 1-round OSM protocol also uses pre-computed randomnesses to mask s and x . Compared to the Beaver-triple-based [7] and oblivious-transfer (OT)-based approaches [52], our protocol saves $\sim 50\%$ of online communication while having the same offline communication and round complexities.

By decomposing the sparse matrix into linear transformations and applying our specialized protocols, our (SM)² protocol reduces the complexity of evaluating $|\mathcal{V}| \times |\mathcal{V}|$ sparse matrices with $|\mathcal{E}|$ non-zero values from $O(|\mathcal{V}|^2)$ to $O(|\mathcal{E}|)$.

1.2 VIRGOS: Secure GCN made Efficient

Supported by our new sparsity techniques, we build VIRGOS, a two-party computation (2PC) framework for GCN inference and training over vertical data. Our contributions include:

- 1) We are the first to explore sparsity over vertically split, secret-shared data in MPC, enabling decompositions of sparse matrices with arbitrary sparsity and isolating computations that can be performed in plaintext without sacrificing privacy.
- 2) We propose two efficient 2PC primitives for OP and OSM, both optimally single-round. Combined with our sparse matrix decomposition approach, our (SM)² protocol ($\Pi_{(\text{SM})^2}$) achieves constant-round communication costs of $O(|\mathcal{E}|)$, reducing memory requirements and avoiding out-of-memory errors for large matrices. In practice, it saves 99%+ communication and reduces $\sim 72\%$ memory usage over large (5000×5000) matrices compared with using Beaver triples.
- 3) We build an end-to-end secure GCN framework for inference and training over vertically split data, maintaining accuracy on par with plaintext computations. We will open-source our evaluation code for research and deployment.

To evaluate the performance of VIRGOS, we conducted extensive experiments over three standard graph datasets (Cora [49], Citeseer [22], and Pubmed [20]), reporting communication, memory usage, accuracy, and running time under varying network conditions, along with an ablation study with or without (SM)². Below, we highlight our key achievements.

Communication (§7.1). VIRGOS saves communication by 50-80% (*cf.*, CoGNN [33], OblivGNN [60]).

Memory usage (§7.2). VIRGOS alleviates out-of-memory problems of using Beaver-triples [7] for large datasets.

Accuracy (§7.3). VIRGOS achieves inference and training accuracy comparable to plaintext counterparts.

Computational efficiency (§7.4). VIRGOS is faster by 6-45% in inference and 28-95% in training across various networks and excels in narrow-bandwidth and low-latency ones.

Table 1: Notation and Definition

$\mathcal{P}_i, \langle \cdot \rangle_i$	Party i and its share ($i \in \{0, 1\}$)
L	The bit-length of data
$\pi, b, U, \langle u \rangle$	Pre-computed randomnesses
δ_x	Masked version of value/vector x
$\mathbb{M}_{m,n}(\mathcal{R})$	A set of $m \times n$ matrices with entries in a ring \mathcal{R}
$M_{m,n}$	A matrix M of size $m \times n$
$M[i, j]$	The value of M at the i -th row and j -th column
σX	Permutation operation σ over a matrix/vector X
\mathbb{S}_n	Permutation group of n elements

Impact of $(SM)^2$ (§7.5). Our $(SM)^2$ protocol shows a 10-42× speed-up for 5000×5000 matrices and saves 10-21% memory for “small” datasets and up to 90%+ for larger ones.

2 Preliminary

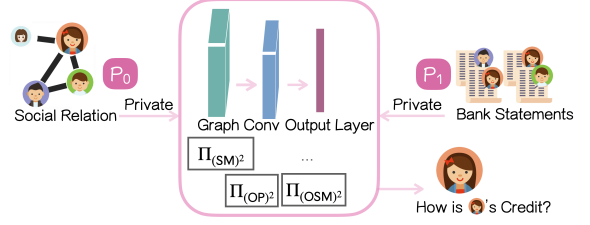
Notations. Table 1 summarizes the main notations. \mathbb{A} denotes an Abelian group. \mathbb{S}_n denotes a permutation group of n elements. $\mathbb{M}_{m,n}(\mathcal{R})$ denotes a matrix ring, which defines a set of $m \times n$ matrices with entries in a ring \mathcal{R} , forming a ring under matrix addition and multiplication. $M_{m \times n} = (M[i, j])_{i,j=1}^{m,n}$ denotes an $m \times n$ matrix² where row indices are $\{1, 2, \dots, m\}$ and column indices are $\{1, 2, \dots, n\}$, and $M[i, j]$ is the value at the i -th row and j -th column. $\Pi(\cdot; \cdot)$ denotes a protocol execution between two parties, \mathcal{P}_0 and \mathcal{P}_1 , where \mathcal{P}_0 's inputs are the left part of ‘;’ and \mathcal{P}_1 's inputs are the right part of ‘;’.

Secret Sharing. We use 2-out-of-2 additive secret sharing over a ring, where the floating-point values are encoded to be fixed-point numbers $x \in \mathbb{Z}/2^f\mathbb{Z}$, with $L = 64$ bits representing decimals and $f = 18$ bits representing the fractional part [38]. Specifically, one party \mathcal{P}_0 holds the share $\langle x \rangle_0 \in \mathbb{Z}$, while the other party \mathcal{P}_1 holds the share $\langle x \rangle_1 \in \mathbb{Z}$ such that $x \cdot 2^f = \langle x \rangle_0 + \langle x \rangle_1$. The shares can be arithmetic or binary.

Graph Convolutional Networks. GCN [31] has been proposed for training over graph data, using graph structure and node features as input. Like most neural networks, GCN consists of multiple linear and non-linear layers. Compared to CNN, GCN replaces convolutional layers with graph convolution layers (more details on GCN architecture and its training/inference are in Section 6). Graph convolution can be computed by SMM, often yielding many 0-value results.

Let $A \in \mathbb{M}_{|\mathcal{V}|,|\mathcal{V}|}(\mathcal{R})$ be a (normalized) adjacency matrix of a graph with $|\mathcal{V}|$ nodes and $X \in \mathbb{M}_{|\mathcal{V}|,d}(\mathcal{R})$ be the feature matrix (with dimensionality d) of the nodes. The graph convolution layer (with output dimensionality k) is defined as $Y = AXW$, where $Y \in \mathbb{M}_{|\mathcal{V}|,k}(\mathcal{R})$ is the output and $W \in \mathbb{M}_{d,k}(\mathcal{R})$ is a trainable parameter. As matrix multiplication costs increase linearly with input size and $k \ll |\mathcal{V}|$ in practice, the challenge of secure GCN lies in the SMM of AX . Multiplying (dense) W can be done using Beaver’s approach.

²For simplicity, we omit the subscript of $M_{m \times n}$ when the values of m and n are clear from the context. Also, we write $M = (M[i, j])_{i,j=1}^n$ if $m = n$.


Figure 1: Ideal Functionality of VIRGOS

3 System Overview and Security Model

3.1 Workflow of VIRGOS

Figure 1 outlines VIRGOS’s function. A graph owner \mathcal{P}_0 , with an adjacency matrix A corresponding to a private graph \mathcal{G} , and a feature owner \mathcal{P}_1 with private node features X , aim to jointly train a GCN without revealing their private inputs. This involves computing a parameterized function $\text{GCN}(A, X; W)$, where the weights W are secret-shared over the two parties.

The VIRGOS framework includes a sparse matrix decomposition method (Section 4) and secure 2PC protocols for permutation (Π_{OP} , Section 5.1), selection-multiplication (Π_{OSM} , Section 5.2), and SMM ($\Pi_{(\text{SM})^2}$, Section 5.3). The sparse matrix decomposition is performed solely by the graph owner, while all 2PC protocols are executed by both parties without disclosing any intermediate computation results.

In practical cross-institution collaboration, graph owners can be social networking platforms (e.g., Facebook) holding social relationships as a graph, and feature owners can be banks holding users’ bank statements as node features. As a motivating example, they may want to build a credit-investigation model for predicting the credit of a loaner for future repayment while keeping their data confidential. Our setting can be extended to multi-party, where different types of node features are learned from different parties (e.g., bank statements from banks and transactions from online-shopping companies). Usually, the graph structure is fixed to represent a specific relationship, such as a social circle, in real-world scenarios. Thus, we focus on single-party graph ownership without limiting feature ownerships. A general case of arbitrary partitioning has been discussed in Section 9.

3.2 Security Model

VIRGOS can be instantiated with any type of security models offered by the corresponding MPC protocols. Following advances [4, 32, 33, 51, 56, 63], VIRGOS focuses on 2PC security against the static semi-honest probabilistic polynomial time (PPT) adversary \mathcal{A} regarding the real/ideal-world simulation paradigm [34]. Specifically, two parties, \mathcal{P}_0 and \mathcal{P}_1 , with inputs $\langle x \rangle_0$ and $\langle x \rangle_1$, want to compute a function $y = f(\langle x \rangle_0, \langle x \rangle_1)$ without revealing anything other than y . \mathcal{A} corrupts either \mathcal{P}_0 or \mathcal{P}_1 at the start, following the protocol, but tries to learn the other’s private inputs. \mathcal{A} can only learn data from the corrupted party but nothing from honest ones.

Many protocols utilize pre-computations for improving efficiency, e.g., Beaver triples [7] for multiplication. They can be realized by a data-independent offline phase run by a semi-honest dealer \mathcal{T} or 2PC protocols from homomorphic encryption [36] or

oblivious transfer [28, 52] or oblivious shuffle [12, 50]. We adopt the first common approach (also called client-aided setting [4]) for simplicity. The \mathcal{T} does not interact with any party (particularly, receives nothing) online. It only generates pseudo-randomnesses in an input-independent offline phase by counter-indexed computations of pseudorandom function (PRF), where \mathcal{T} and \mathcal{P}_i share a PRF key (denoted by key_i) for $i \in \{0, 1\}$ and a counter ctr are synchronized among all parties. We defer the explicit functionality definitions and security proofs of our protocols to Appendix E.

3.3 Scope of Graph Protection

Like existing MPC works, VIRGOS protects the entry values stored in the graph and (intermediate) computations. For metadata, most secure matrix multiplication protocols (without sparse structure) reveal input dimensionality (e.g., $|\mathcal{V}|$ in GCN) that is typically considered public knowledge. When sparsity is explored, it is normal to leak reasonable knowledge, such as $|\mathcal{V}| + |\mathcal{E}|$ in GraphSC [40]. In VIRGOS, the only additional metadata revealed is $|\mathcal{E}|$ that has been comprehensively explained in §5.3. This leakage is tolerable (and unavoidable) since the efficiency gain is correlated to $|\mathcal{E}|$. Corresponding to VIRGOS's GCN training, the *dimension* of adjacency matrix A (i.e., equal to $|\mathcal{V}|$) and the *dimension* of feature matrix X are assumed to be public.

Privacy leakages from training/inference results, e.g., embedding inversion and sensitive attribute inference, also appear in plaintext computations and are beyond our scope. These can be protected via orthogonal techniques like (local) differential privacy and robustness training, which are compatible with our work. In the semi-honest settings, the attacker can only view the well-formed secret shares and not actively perform the malicious attacks like model inversion.

4 Sparse Matrix Decomposition

Graph convolution layers AXW encode the graph structures in A into GCNs. Graph convolution is then computed by SMM AX . By bridging computations of matrices and graphs, we detail how to decompose a sparse matrix A into a product of special matrices for more efficient SMM. In essence, we *revisit linear algebra* relations to *faithfully* capture the graph.

4.1 Bipartite Graph Representation

We represent graph \mathcal{G} corresponding to A as bipartite graphs, and decompose A into matrices. This bipartite representation enables the identification of structured patterns that facilitate efficient SMM aligning with our 2PC protocols.

Graph Decomposition via Edges. Non-zero entries in A correspond to edges between nodes in \mathcal{G} . By representing \mathcal{G} as two bipartite graphs— \mathcal{G}_{out} (the out-degree node-to-edge relation) and \mathcal{G}_{in} (the in-degree edge-to-node relation)—we can decompose A into the product $A_{\text{out}}A_{\text{in}}$, where A_{out} and A_{in} reflect the respective bipartite structures are sparse matrices correspond to \mathcal{G}_{out} and \mathcal{G}_{in} , respectively. Consider graph \mathcal{G} (with arbitrary-sparse A) in Figure 2a. We label each edge and treat them as imaginary nodes (' \diamond ' drawn by dotted lines) to construct \mathcal{G}_{out} and \mathcal{G}_{in} as in Figure 2b. This representation decomposes A into $A_{\text{out}}A_{\text{in}}$ as in Figure 3.

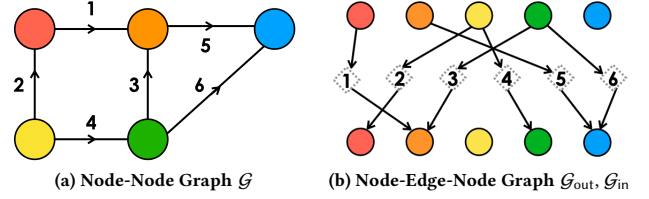


Figure 2: Graph Decomposition through Edges

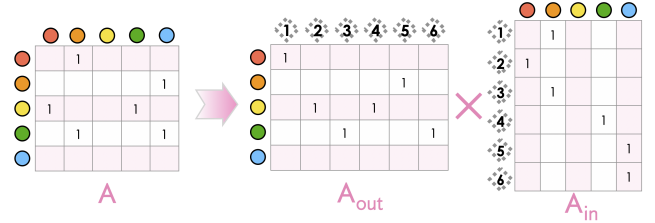


Figure 3: Matrix Decomposition Equivalent to Figure 2

4.2 Permutation for Monotonicity

A_{out} and A_{in} are still unstructured sparse matrices, challenging further decomposition. We then permute the columns of A_{out} and the rows of A_{in} to yield permuted matrices A'_{out} and A'_{in} with monotonically non-decreasing (row-index, column-index) coordinates for non-zero positions as shown in Figure 4. Definitions 1 and 2 formulate P-type and Q-type sparse matrices to capture these monotonic relations, where P-type matrices have exactly one non-zero value in each column, and Q-type matrices have exactly one non-zero value in each row. Note that $A \neq A'_{\text{out}}A'_{\text{in}}$ as the imaginary nodes in A'_{out} and A'_{in} are ordered differently. We use a permutation σ_3 (before defining σ_1, σ_2) to map these nodes for preserving the topology among edges and decomposing A , given by $A'_{\text{out}}\sigma_3A'_{\text{in}}$.

Recall that A is a normalized adjacency matrix, i.e., its non-zero values may not be 1. To account for this, we introduce a diagonal matrix Λ in the decomposition to store the non-zero edge weights. Theorem 1 (proven in §B.1) shows that any sparse matrix A can be decomposed to a P-type matrix, a diagonal matrix, a permutation, and a Q-type matrix.

THEOREM 1. *Let $A \in \mathbb{M}_{m,n}(\mathcal{R})$ be an $m \times n$ matrix, where each entry is an element from ring \mathcal{R} . The elements of A are 0's except t of them. There exists a matrix decomposition $A = A'_{\text{out}}\Lambda\sigma_3A'_{\text{in}}$, where $A'_{\text{out}} \in \mathbb{M}_{m,t}(\mathcal{R})$ is a P-type matrix, $\Lambda \in \mathbb{M}_{t,t}(\mathcal{R})$ is a diagonal matrix, $\sigma_3 \in \mathbb{S}_t$ is a permutation, and $A'_{\text{in}} \in \mathbb{M}_{t,n}(\mathcal{R})$ is a Q-type matrix.*

4.3 Re-decomposition to Basic Operations

Given the permuted matrices A'_{out} and A'_{in} with the monotonicity properties, we can re-decompose them into a product of permutation, diagonal, and constant matrices. Due to the page limit, we focus on the intuition of re-decomposing A'_{in} (Q-type matrix)³ and

³We can view a P-type matrix (e.g., A'_{out}) as a transpose of a Q-type matrix and perform re-decomposition similarly.

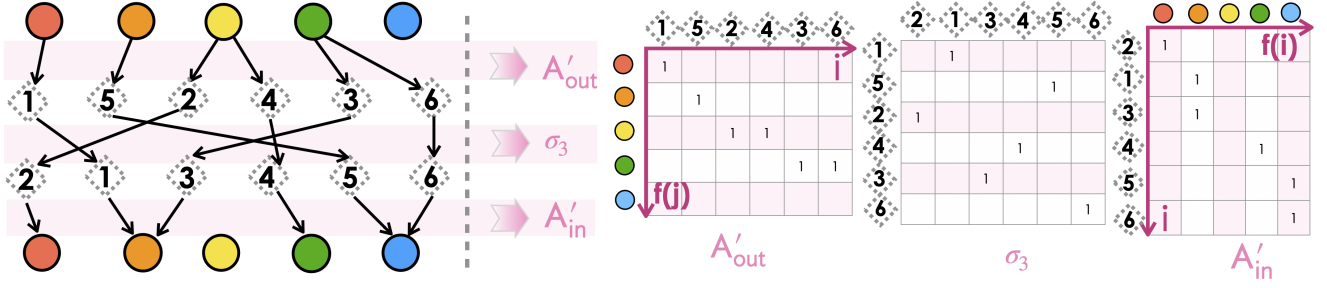
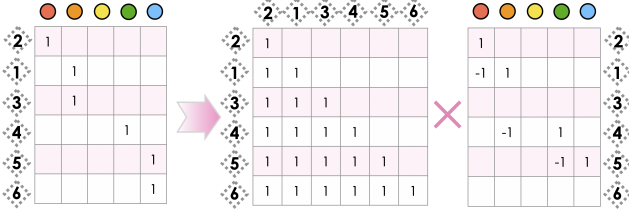


Figure 4: Graph/Matrix Decomposition with Monotonicity


 Figure 5: Decomposition of $A'_{in} = \Sigma \delta'$

the general theorem. Implementation details and proofs can be found in Appendices B and C.

We consider two constant lower triangular matrices:

- 1) a “summation matrix” $\Sigma \in \mathbb{M}_{t,t}(\mathcal{R})$ with $\Sigma[i, j] = 1$ if $i \geq j$ or 0 otherwise;
- 2) a “difference matrix” $\delta_k \in \mathbb{M}_{k,k}(\mathcal{R})$ with $\delta_k[i, j] = 1$ for $i = j$ or -1 for $j = i - 1$, or 0 otherwise.

Intuitively, when multiplying with a (column) vector, Σ sums values on or above each element, while δ_k computes a difference between each element and its previous one.

Based on the above intuition, it is not hard to decompose A'_{in} into a product of Σ and another matrix δ' (Figure 5). Interestingly, we observe that the resulting matrix δ' “contains” a difference matrix (with size equals the number of non-zero columns in A'_{in}) on its left-top corner (after permuting its rows and columns). This relation can be characterized by expressing δ' into a product of permutation (σ_1, σ_2), diagonal (Γ_{in}), and difference (δ) matrices, as in Figure 6.

General Theorem. Combining Theorem 1 and matrix decomposition of Q-type (Theorem 4 proved in §B.4) and P-type (Theorem 5 proved in §B.5) matrices, Theorem 2 concludes the general matrix decomposition (proof in §B.2). Essentially, an arbitrary-sparse matrix can be transformed into a sequence of permutation and matrix multiplication.

THEOREM 2 (SPARSE MATRIX DECOMPOSITION). *Let an $m \times n$ sparse matrix $A \in \mathbb{M}_{m,n}(\mathcal{R})$ contain n_{row} non-zero rows, n_{col} non-zero columns, and t non-zero elements. Then, there exists a matrix decomposition $A = \sigma_5 \delta_m^T \Gamma_{out} \sigma_4 \Sigma^T \Lambda \sigma_3 \Sigma \sigma_2 \Gamma_{in} \delta_n \sigma_1$, where $\sigma_5 \in \mathbb{S}_m$, $\sigma_4 \in \mathbb{S}_t$, $\sigma_3 \in \mathbb{S}_t$, $\sigma_2 \in \mathbb{S}_t$, $\sigma_1 \in \mathbb{S}_n$, and,*

- 1) $\Sigma = (\Sigma[i, j])_{i,j=1}^t$ is the left-down triangle matrix such that $\Sigma[i, j] = 1$ if $i \geq j$ or 0 otherwise,
- 2) $\delta_k = (\delta_k[i, j])_{i,j=1}^k$ is the left-down triangle matrix such that

$$\delta_k[i, j] = 1 \text{ for } i = j \text{ or } -1 \text{ for } j = i - 1, \text{ or } 0 \text{ otherwise,}$$

$$3) \Gamma_{in} = (\Gamma_{in}[i, j])_{i=1, j=1}^{t,n} \text{ is a matrix such that } \Gamma_{in}[i, j] = 1 \text{ for } 1 \leq i = j \leq n_{col} \text{ or } 0 \text{ otherwise,}$$

$$4) \Gamma_{out} = (\Gamma_{out}[i, j])_{i=1, j=1}^{m,t} \text{ is a matrix such that } \Gamma_{out}[i, j] = 1 \text{ for } 1 \leq i = j \leq n_{row} \text{ or } 0 \text{ otherwise.}$$

4.4 Reasoning from Graph Perspective

To illustrate the sparse matrix decomposition underlying Theorem 2 for arbitrary topology, Figure 7 shows the directed edges in a reversed direction represented by the decomposed matrices in Figure 6 and recovers the original \mathcal{G}_{in} . Consider a vector $X = [x_1, x_2, x_3, x_4, x_5]^T$, which passes 5 values through graph \mathcal{G}_{in} (equivalent to SMM $A'_{in} X$). After σ_1 operation, X passes from $\{\bullet, \bullet, \bullet, \bullet, \bullet\}$ to the re-ordered $\{\bullet, \bullet, \bullet, \bullet, \bullet\}$. Then, the δ operation computes the difference of values stored in the neighboring source nodes to obtain the target nodes.

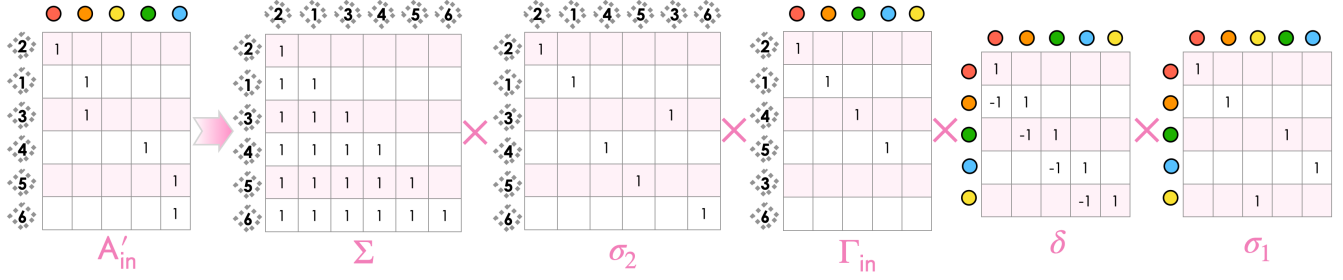
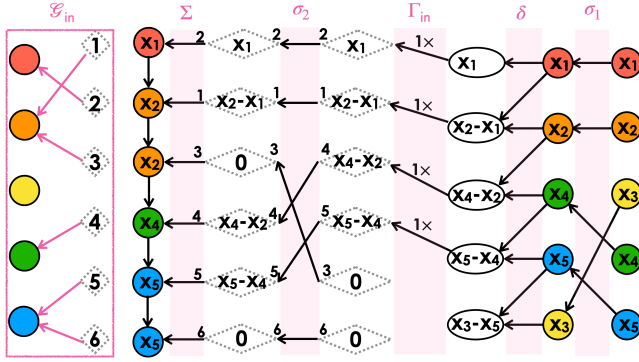
The Γ_{in} operation extracts the effective message passing to the subsequent graph computation by classifying the nodes with or without in-degree edges in \mathcal{G}_{in} . Thus, all interdependent nodes $\{x_1(\bullet), x_2(\bullet), x_4(\bullet), x_5(\bullet)\}$ in \mathcal{G}_{in} are recovered, *i.e.*, those nodes containing one or multiple in-degree edges.

After the σ_2 operation, nodes are rearranged in order $\{x_1(\bullet), x_2(\bullet), x_3(\text{None}), x_4(\bullet), x_5(\bullet)\}$. Interestingly, the imaginary nodes (\circ drawn by dotted lines) reflect the δ' matrix in Figure 5. Next, the Σ operation takes the sum of source nodes to get target nodes. Finally, we get the results $\{\bullet, \bullet, \bullet, \bullet, \bullet\}$, which recover the (permuted) in-degree edges (represented by A'_{in}) matching the correct nodes in \mathcal{G}_{in} .

5 Secure Sparse Matrix Multiplication

Given the sparse matrix decomposition from Theorem 2, SMM can be transformed into an ordered sequence of basic operations from right to left as Theorem 3 (proof in §B.3). If we expect to compute XA , the linear transformations should be performed sequentially from left to right. For a sparse matrix that is multiplied by another sparse matrix, we can combine the sequential computation of AX and XA .

THEOREM 3 (SPARSE MATRIX MULTIPLICATION). *Consider a sparse matrix A and a dense matrix X . Computing $AX = \sigma_5 \delta_m^T \Gamma_{out} \sigma_4 \Sigma^T \Lambda \sigma_3 \Sigma \sigma_2 \Gamma_{in} \delta_n \sigma_1 X$ requires an ordered sequence of permutation group action, element-wise multiplication, and constant matrix multiplication from right to left.*

Figure 6: Re-decomposition of A'_{in} (Q-type Matrix)Figure 7: Recover In-degrees in G_{in} through $A'_{in} X$

For secure MPC, the graph owner \mathcal{P}_0 first decomposes its graph to obtain matrices $\sigma_1, \sigma_2, \sigma_3, \sigma_4, \sigma_5, \Gamma_{out}, \Gamma_{in}, \Lambda$. These matrices are privacy-sensitive and should not be learned by the feature owner \mathcal{P}_1 . The summation matrix Σ and difference matrices δ_m, δ_n are constants (given dimensionality of A) and thus are public to both \mathcal{P}_0 and \mathcal{P}_1 . Next, \mathcal{P}_0 and \mathcal{P}_1 jointly execute the MPC protocols of SMM, which multiplies the above matrices described in Theorem 3.

We first present an oblivious permutation protocol (for secure permutation operations based on $\sigma_1, \dots, \sigma_5$) in Section 5.1 and then an oblivious selection-multiplication protocol (for privately multiplying Γ_{out} and Γ_{in}) in Section 5.2. Finally, we describe how to realize our $(SM)^2$ protocol using our OP and OSM protocols in Section 5.3.

5.1 Oblivious Permutation

Protocol Π_{OP} is our oblivious permutation protocol. Given \mathcal{P}_0 's private permutation $\sigma \in \mathbb{S}_k$ and \mathcal{P}_1 's private k -dimensional vector $X \in \mathbb{Z}_{2^L}^k$, Π_{OP} generates a secret share $\langle \sigma X \rangle_i$ for $\mathcal{P}_i \in \{\mathcal{P}_0, \mathcal{P}_1\}$ without revealing σ or X . The protocol parameter type $\in \{\text{plain}, \text{shared}\}$ specifies the type of input vector X . If type is plain, X is initially owned by \mathcal{P}_1 ; otherwise, it is secret-shared among \mathcal{P}_0 and \mathcal{P}_1 .

Offline Phase. The commodity server \mathcal{T} assists \mathcal{P}_0 and \mathcal{P}_1 to generate a random permutation $\pi \in \mathbb{S}_k$, a random vector $U \in \mathbb{Z}_{2^L}^k$, and correlated randomnesses $\langle \pi U \rangle_0 \in \mathbb{Z}_{2^L}^k, \langle \pi U \rangle_1 \in \mathbb{Z}_{2^L}^k$.

Online Phase. \mathcal{P}_0 masks σ using random π^{-1} (i.e., inverse permutation of π) to get random δ_σ (Line 6). If type is plain, \mathcal{P}_1 masks

Protocol 1 Π_{OP} : Oblivious Permutation

Parameter: \mathcal{P}_0 and \mathcal{P}_1 know type $\in \{\text{plain}, \text{shared}\}$.
Input: \mathcal{P}_0 inputs σ and \mathcal{P}_1 inputs X if type == plain; otherwise, \mathcal{P}_0 inputs $(\sigma, \langle X \rangle_0)$ and \mathcal{P}_1 inputs $\langle X \rangle_1$.
Output: \mathcal{P}_0 gets $\langle \sigma X \rangle_0$ and \mathcal{P}_1 gets $\langle \sigma X \rangle_1$.

- 1: // Offline Phase: Generate Correlated Randomness
- 2: $\mathcal{T}, \mathcal{P}_0$: Get $\pi, \langle \pi U \rangle_0 \leftarrow \text{PRF}(\text{key}_0, \text{ctr})$
- 3: $\mathcal{T}, \mathcal{P}_1$: Get $U \leftarrow \text{PRF}(\text{key}_1, \text{ctr})$
- 4: \mathcal{T} : Send $\langle \pi U \rangle_1 = \pi U - \langle \pi U \rangle_0$ to \mathcal{P}_1
- 5: // Online Phase: Compute $\langle \sigma X \rangle$ in 1 Round
- 6: \mathcal{P}_0 : Send $\delta_\sigma = \sigma \cdot \pi^{-1}$ to \mathcal{P}_1
- 7: **if** type == plain **then**
- 8: \mathcal{P}_1 : Send $\delta_X = X - U$ to \mathcal{P}_0
- 9: \mathcal{P}_0 : Compute $\langle \sigma X \rangle_0 = \sigma \delta_X + \delta_\sigma \langle \pi U \rangle_0$
- 10: **else**
- 11: \mathcal{P}_1 : Send $\delta_{\langle X \rangle_1} = \langle X \rangle_1 - U$ to \mathcal{P}_0
- 12: \mathcal{P}_0 : Compute $\langle \sigma X \rangle_0 = \sigma \delta_{\langle X \rangle_1} + \delta_\sigma \langle \pi U \rangle_0 + \sigma \langle X \rangle_0$
- 13: **end if**
- 14: \mathcal{P}_1 : Compute $\langle \sigma X \rangle_1 = \delta_\sigma \langle \pi U \rangle_1$
- 15: **return** $\langle \sigma X \rangle$

Table 2: Communication for Oblivious Permutation

Protocol	Offline	Online	Round
Asharov <i>et al.</i> [2]	0	$6kL$	3
OLGA [4]	$2k(L + 32)$	$2kL$	1
Araki <i>et al.</i> [1]	0	$4kL$	2
Π_{OP}	kL	$kL + k \log k$	1

L : bit-length of data, k : degree of the permutation group

X using random U to get δ_X (Line 8). If type is shared, \mathcal{P}_1 needs not mask X since $\langle X \rangle_0$ is kept by \mathcal{P}_0 as a part of computing $\langle \sigma X \rangle_0$ (Line 12). In this case, \mathcal{P}_1 masks $\langle X \rangle_1$ using random U to get random $\delta_{\langle X \rangle_1}$ (Line 11). \mathcal{P}_0 and \mathcal{P}_1 can then obtain the respective secret shares $\langle \sigma X \rangle_0, \langle \sigma X \rangle_1$.

Correctness. Here, we verify that $\langle \sigma X \rangle_0 + \langle \sigma X \rangle_1 = \sigma X$. If type is plain, it holds that $\sigma X = \sigma(X - U + U) = \sigma(\delta_X + U) = \sigma \delta_X + \sigma U = \sigma \delta_X + \sigma \pi^{-1} \pi U = \sigma \delta_X + \delta_\sigma \pi U = \sigma \delta_X + \delta_\sigma \langle \pi U \rangle_0 + \delta_\sigma \langle \pi U \rangle_1$.

If X 's type is shared, $\sigma X = \sigma(\langle X \rangle_0 + \langle X \rangle_1 - U + U) = \sigma(\langle X \rangle_0 + \delta_{\langle X \rangle_1} + U) = \sigma \langle X \rangle_0 + \sigma \delta_{\langle X \rangle_1} + \sigma \pi^{-1} \pi U = \sigma \langle X \rangle_0 + \sigma \delta_{\langle X \rangle_1} + \delta_\sigma \pi U = \sigma \langle X \rangle_0 + \sigma \delta_{\langle X \rangle_1} + \delta_\sigma \langle \pi U \rangle_0 + \delta_\sigma \langle \pi U \rangle_1$.

Protocol 2 Π_{OSM} : Oblivious Selection-Multiplication

Input: \mathcal{P}_0 inputs $(s, \langle x \rangle_0)$ and \mathcal{P}_1 inputs $\langle x \rangle_1$.

Output: \mathcal{P}_0 gets $\langle sx \rangle_0$ and \mathcal{P}_1 gets $\langle sx \rangle_1$.

- 1: // Offline Phase: Generate Correlated Randomness
 - 2: $\mathcal{T}, \mathcal{P}_0$: Get $(b, \langle u \rangle_0, \langle bu \rangle_0) \leftarrow \text{PRF}(\text{key}_0, \text{ctr})$
 - 3: $\mathcal{T}, \mathcal{P}_1$: Get $\langle u \rangle_1 \leftarrow \text{PRF}(\text{key}_1, \text{ctr})$
 - 4: \mathcal{T} : Send $\langle bu \rangle_1 = bu - \langle bu \rangle_0$ to \mathcal{P}_1
 - 5: // Online Phase: Compute $\langle sx \rangle$ in 1 Round
 - 6: \mathcal{P}_0 : Send $\delta_s = s - b$ to \mathcal{P}_1
 - 7: \mathcal{P}_1 : Send $\delta_{\langle x \rangle_1} = \langle x \rangle_1 - \langle u \rangle_1$ to \mathcal{P}_0
 - 8: \mathcal{P}_0 : Compute $\delta_x = \langle x \rangle_0 - \langle u \rangle_0 + \delta_{\langle x \rangle_1}$
 - 9: \mathcal{P}_0 : Compute $\langle sx \rangle_0 = s\delta_x + \delta_s \langle u \rangle_0 + (-1)^{\delta_s} \langle bu \rangle_0$
 - 10: \mathcal{P}_1 : Compute $\langle sx \rangle_1 = \delta_s \langle u \rangle_1 + (-1)^{\delta_s} \langle bu \rangle_1$
 - 11: **return** $\langle sx \rangle$
-

Table 3: Communication for Oblivious Selection-Mult.

Protocol	Offline	Online	Round
Π_{Mult} [7]	L	$2L$	1
OT [52]	L	$2L + 1$	1
Π_{OSM}	L	$L + 1$	1

 L : bit-length of data

Communication. Since $\sigma \in \mathbb{S}_k$, $\log k$ bits are enough to represent k elements. The online phase of Π_{OP} requires communication of $k \log k + kL$ bits (i.e., sending δ_σ, δ_X in the plain case or sending $\delta_\sigma, \delta_{\langle X \rangle_1}$ in the shared case) in 1 round.

Comparison to Existing Works. Asharov *et al.* [2] spend $6kL$ bits online in three rounds. Araki *et al.* [1]’s oblivious shuffle requires $4kL$ bits in two rounds for k -element permutation. The OLGA protocol [4] is 1-round but communicates $2k(L + 32)$ bits offline and $2kL$ bits online. Our Π_{OP} protocol is also 1-round, communicates kL bits offline and $kL + k \log k$ bits online. Particularly, k equals to $|\mathcal{E}|$ or $|\mathcal{V}|$ for GCN. In practice, $\log k$ is much smaller than L , e.g., for a 10^6 -node graph, $\log k = 20 < L = 64$.

5.2 Oblivious Selection-Multiplication

We design the oblivious selection-multiplication protocol Π_{OSM} in Protocol 2. It takes a private bit (called “selector”) $s \in \mathbb{Z}_2$ from \mathcal{P}_0 and a secret share $\langle x \rangle$ of an arithmetic number $x \in \mathbb{Z}_{2L}$ owned by \mathcal{P}_0 and \mathcal{P}_1 . Π_{OSM} generates a secret share of 0 if $s = 0$ or share of x otherwise without disclosing s or x .

Offline Phase. The commodity server \mathcal{T} assists $\mathcal{P}_0, \mathcal{P}_1$ to generate a random bit $b \in \mathbb{Z}_2$, a secret share of a random number $u \in \mathbb{Z}_{2L}$, and correlated randomness $\langle bu \rangle_0 \in \mathbb{Z}_{2L}, \langle bu \rangle_1 \in \mathbb{Z}_{2L}$.

Online Phase. \mathcal{P}_0 masks s using random b to generate random δ_s (Line 6). \mathcal{P}_1 masks $\langle x \rangle_1$ using random $\langle u \rangle_1$ to generate random $\delta_{\langle x \rangle_1}$ (Line 7). After receiving the masked $\langle x \rangle_1$ and s , \mathcal{P}_0 and \mathcal{P}_1 can respectively compute the shares $\langle sx \rangle_0, \langle sx \rangle_1$.

Correctness. Here, we verify that $\langle sx \rangle_0 + \langle sx \rangle_1 = sx$ by using Lemma 1 (proven in Appendix D).

Lemma 1. Let \mathbb{A} be an Abelian group and $\mathbb{B} = \{0, 1\}$ be the binary group. Let map $f : \mathbb{B} \times \mathbb{A} \rightarrow \mathbb{A}$ be defined as $f(s, x) = x$ if $s = 1$ else 0. Then, for any $s, b \in \mathbb{B}$ and $x, u \in \mathbb{A}$:

- (i) $f(s, x + u) = f(s, x) + f(s, u)$.
- (ii) $f(s + b, x) = f(s, x) + (-1)^s f(b, x)$.

Let $f : \mathbb{B} \times \mathbb{A} \rightarrow \mathbb{A}$ be the same f as above. Using Lemma 1, we have $f(s, x) = f(s, x - u) + f(s, u) = f(s, \delta_x) + f(s - b + b, u) = f(s, \delta_x) + f(\delta_s, u) + (-1)^{\delta_s} f(b, u) = s\delta_x + \delta_s u + (-1)^{\delta_s} \langle bu \rangle_0 = s\delta_x + \delta_s \langle u \rangle_0 + \delta_s \langle u \rangle_1 + (-1)^{\delta_s} \langle bu \rangle_0 + (-1)^{\delta_s} \langle bu \rangle_1$.

Communication. Π_{OSM} requires communicating $L + 1$ bits (i.e., 65 bits for sending $\delta_{\langle x \rangle_1}, \delta_s$) online in 1 round. Except for Π_{OSM} , OT based [52] protocol (by using two OT instances to select $\langle x \rangle$ and 0) and standard arithmetic multiplication (by transforming binary $s \in \mathbb{Z}_2$ into arithmetic $s \in \mathbb{Z}_{2L}$) can also realize the functionality of section-multiplication. As compared in Table 3, our protocol saves about 50% of communication while having the same round complexity compared to the OT-based [52] protocol and standard Beaver-triple-based [7] (Π_{Mult}).

5.3 Construction of $(\text{SM})^2$

Based on our sparse matrix decomposition and protocols for OP and OSM, we present our $(\text{SM})^2$ protocol $\Pi_{(\text{SM})^2}$ in Protocol 3. It takes a sparse matrix $A \in \mathbb{M}_{m,n}(\mathcal{R})$ from \mathcal{P}_0 and a dense matrix $X \in \mathbb{M}_{n,d}(\mathcal{R})$ from \mathcal{P}_1 . $\Pi_{(\text{SM})^2}$ generates a secret share $\langle AX \rangle_i$ for $\mathcal{P}_i \in \{\mathcal{P}_0, \mathcal{P}_1\}$ without leaking A or X .

$(\text{SM})^2$ Realization. Following Theorem 3, $\Pi_{(\text{SM})^2}$ essentially performs an ordered sequence of linear transformations $(\sigma_5 \delta_m^T \Gamma_{\text{out}} \sigma_4 \Sigma^T \Lambda \sigma_3 \Sigma \sigma_2 \Gamma_{\text{in}} \delta_n \sigma_1)$ from right to left over \mathcal{P}_1 ’s private input X . Multiplying public matrices $\delta_n, \Sigma, \Sigma^T, \delta_m^T$ can be done non-interactively on secret shares (Lines 3, 6, 9, 12).

Permuting the rows of input X or intermediate output Y based on $\sigma_1, \dots, \sigma_5$ are performed by invoking d parallel Π_{OP} instances as Π_{OP} takes a column vector as input, but X and Y are matrices with d columns (Lines 2, 5, 7, 10, 13).

Since Γ_{in} and Γ_{out} are diagonal matrices with binary values, multiplications of them (Lines 4 and 11) can be done by nd and md parallel Π_{OSM} instances, respectively.⁴ Multiplication of Λ , a diagonal matrix with arithmetic values, is performed similarly, but we can use the standard Beaver-triple-based multiplication protocol Π_{Mult} (Line 8) instead of Π_{OSM} .

Graph Protection and Dimensions. All entries of $\sigma_5, \sigma_4, \sigma_3, \sigma_2, \sigma_1, \Gamma_{\text{out}}, \Gamma_{\text{in}}$, and Λ are protected in $\Pi_{(\text{SM})^2}$. The dimensions of σ_1 and σ_5 are $|\mathcal{V}|$, corresponding to the number of rows in A and X . Since A and X are held by \mathcal{P}_0 and \mathcal{P}_1 , respectively, the dimensions of σ_1 and σ_5 are considered reasonable public knowledge. The dimensions of $\sigma_4, \sigma_3, \sigma_2$, and Λ are $|\mathcal{E}|$, representing tolerable leakage useful for sparsity exploration. Γ_{in} has dimensions of $|\mathcal{E}| \times |\mathcal{V}|$, while Γ_{out} is $|\mathcal{V}| \times |\mathcal{E}|$, both of which do not incur extra graph leakage beyond $|\mathcal{E}|$ or $|\mathcal{V}|$. Importantly, such general statistical information about

⁴In practice, the parties need to pad zero values (non-interactively) before invoking the first Π_{OSM} and cutting off zero values after invoking the last Π_{OSM} to ensure consistent matrix dimensionality. For simplicity, we omit this step in our $\Pi_{(\text{SM})^2}$ protocol presentation.

Protocol 3 $\Pi_{(SM)^2}$: Secure Sparse Matrix Multiplication**Input:** \mathcal{P}_0 inputs A and \mathcal{P}_1 inputs X .**Output:** \mathcal{P}_0 gets $\langle Y \rangle_0$ and \mathcal{P}_1 gets $\langle Y \rangle_1$ where $Y = AX$.

- 1: \mathcal{P}_0 : Decomposes $A = \sigma_5 \delta_m^T \Gamma_{out} \sigma_4 \Sigma^T \Lambda \sigma_3 \Sigma \sigma_2 \Gamma_{in} \delta_n \sigma_1$
- 2: $\mathcal{P}_0, \mathcal{P}_1$: Invoke $\langle Y \rangle \leftarrow \Pi_{OP}(\sigma_1; X)$ // type == plain
- 3: $\mathcal{P}_0, \mathcal{P}_1$: Locally compute $\langle Y \rangle = \delta_n \langle Y \rangle$
- 4: $\mathcal{P}_0, \mathcal{P}_1$: Invoke $\langle Y \rangle \leftarrow \Pi_{OSM}(\Gamma_{in}, \langle Y \rangle_0; \langle Y \rangle_1)$
- 5: $\mathcal{P}_0, \mathcal{P}_1$: Invoke $\langle Y \rangle \leftarrow \Pi_{OP}(\sigma_2, \langle Y \rangle_0; \langle Y \rangle_1)$
- 6: $\mathcal{P}_0, \mathcal{P}_1$: Locally compute $\langle Y \rangle = \Sigma \langle Y \rangle$
- 7: $\mathcal{P}_0, \mathcal{P}_1$: Invoke $\langle Y \rangle \leftarrow \Pi_{OP}(\sigma_3, \langle Y \rangle_0; \langle Y \rangle_1)$
- 8: $\mathcal{P}_0, \mathcal{P}_1$: Invoke $\langle Y \rangle \leftarrow \Pi_{Mult}(\Lambda, \langle Y \rangle_0; \langle Y \rangle_1)$
- 9: $\mathcal{P}_0, \mathcal{P}_1$: Locally compute $\langle Y \rangle = \Sigma^T \langle Y \rangle$
- 10: $\mathcal{P}_0, \mathcal{P}_1$: Invoke $\langle Y \rangle \leftarrow \Pi_{OP}(\sigma_4, \langle Y \rangle_0; \langle Y \rangle_1)$
- 11: $\mathcal{P}_0, \mathcal{P}_1$: Invoke $\langle Y \rangle \leftarrow \Pi_{OSM}(\Gamma_{out}, \langle Y \rangle_0; \langle Y \rangle_1)$
- 12: $\mathcal{P}_0, \mathcal{P}_1$: Locally compute $\langle Y \rangle = \delta_m^T \langle Y \rangle$
- 13: $\mathcal{P}_0, \mathcal{P}_1$: Invoke $\langle Y \rangle \leftarrow \Pi_{OP}(\sigma_5, \langle Y \rangle_0; \langle Y \rangle_1)$
- 14: **return** $\langle Y \rangle$

Table 4: Cost for $(SM)^2$ on $A \in \mathbb{M}_{m,n}(\mathcal{R})$ and $X \in \mathbb{M}_{n,d}(\mathcal{R})$

Protocol	Offline	Online	Rd
$5 \Pi_{OP}$	$(3t + m + n)dL$	$((3t + m + n)L + 3t \log t + m \log m + n \log n)d$	5
$2 \Pi_{OSM}$	$(m + n)dL$	$((m + n)L + m + n)d$	2
$1 \Pi_{Mult}$	tdL	$2tdL$	1
$\Pi_{(SM)^2}$	$2(2t + m + n)dL$	$((5t + 2m + 2n)L + 3t \log t + m \log m + n \log n + m + n)d$	8

t : number of non-zero elements in A , L : bit-length of data,
 d : node feature dimensionality, Rd: round

the graph does not compromise the privacy of specific nodes or edges or incur identifiable risks.

Correctness. $\Pi_{(SM)^2}$ follows the same sequence of transformations as in Theorem 3, which shows the correctness of our sparse matrix decomposition. Since the underlying Π_{OP} and Π_{OSM} protocols are correct, so does our $\Pi_{(SM)^2}$ protocol.

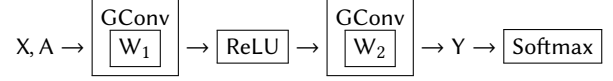
Communication. $\Pi_{(SM)^2}$ invokes $5 \Pi_{OP}$, $2 \Pi_{OSM}$, and $1 \Pi_{Mult}$, communicating $2(2t + m + n)dL$ bits offline and $((5t + 2m + 2n)L + 3t \log t + m \log m + n \log n + m + n)d$ bits online in 8 rounds (see Table 4 for a breakdown). The Beaver-triple-based protocol Π_{Mult} [7] for (dense) matrix multiplication communicates $mndL$ bits offline and $2mndL$ bits online.

In practical GCN usages, we have $m = n = |\mathcal{V}| < t = |\mathcal{E}| \ll |\mathcal{V}|^2 = mn$ and $\log m, \log n, \log t < L = 64$. Also, d is a relatively small constant. So, the communication cost of $\Pi_{(SM)^2}$ is simplified to $O(|\mathcal{E}|)$, rather than $O(|\mathcal{V}|^2)$, by directly using Π_{Mult} for each entry in SMM.

6 End-to-End GCN Inference and Training

Implementation. VIRGOS adopts classical GCN [31] in the transductive setting with two graph convolution layers (GConv) followed by ReLU and softmax function. We implement VIRGOS using

Python in the TensorFlow framework.



We implemented all the above protocols (detailed in Appendix C) in VIRGOS upon secure computation with secret shares. Since GCN inherits conventional neural networks, we still rely on similar functions and layers. Following the ideas of [3, 38, 46, 56, 62], we re-implemented the relevant protocols under the 2PC setting in VIRGOS for ReLU, softmax, Adam optimization, and more. For non-sparse multiplication, VIRGOS still uses Beaver triples [7].

Forward Propagation. Recall that \mathcal{P}_0 holds the (normalized) adjacency matrix A and \mathcal{P}_1 holds the features X . The first GCN layer is defined as $Z = \text{ReLU}(AXW)$, thus \mathcal{P}_0 and \mathcal{P}_1 jointly execute $\Pi_{(SM)^2}$, Π_{Mult} , and ReLU protocols (combining PPA [6], GMW [24], and OSM). \mathcal{P}_0 and \mathcal{P}_1 will get $\langle Z \rangle_0$ and $\langle Z \rangle_1$, respectively. Then, \mathcal{P}_0 and \mathcal{P}_1 securely compute $Y = AZW$ and $\text{Softmax}(Y)$ in the second layer. In the output layer, \mathcal{P}_0 and \mathcal{P}_1 jointly execute secure softmax protocol [62].

Backward Propagation. \mathcal{P}_0 and \mathcal{P}_1 securely compute $\text{softmax}(Y) - Y'$ using cross-entropy loss to get $\frac{\partial \text{loss}}{\partial Y}$, where Y' is the label matrix. Then, we compute the gradient of a graph layer $\frac{\partial \text{loss}}{\partial W} = Z^T A^T \frac{\partial \text{loss}}{\partial Y}$, where the multiplication of $Z^T A^T$ is $(SM)^2$. If we use the SGD optimizer, W is updated to be $W \leftarrow W - \eta \frac{\partial \text{loss}}{\partial W}$, where η is the learning rate. If we use the Adam optimizer [30], W is updated by following the computation of Adam given $\frac{\partial \text{loss}}{\partial W}$. The last step is to securely compute the gradient of ReLU and graph layer similarly.

GCN Inference and Training. As for end-to-end secure GCN computations, \mathcal{P}_0 and \mathcal{P}_1 collaboratively execute a sequence of protocols to run a single forward propagation (for inference) or forward and backward propagation iteratively (for training). VIRGOS supports both single-server simulation for multiple hosts and multiple-server execution in a distributed setting. Using VIRGOS, researchers and practitioners can realize various GCNs using the template of `class SGCN` (Appendix C), similar to using the TensorFlow framework except that *all computations are over secret shares*.

7 Experiments and Evaluative Results

We evaluate the performance of our $(SM)^2$ protocol and VIRGOS's private GCN inference/training on three Ubuntu servers with 16-core Intel(R) Xeon(R) Platinum 8163 2.50GHz CPUs of 62GB RAM and NVIDIA-T4 GPU of 16GB RAM. We aim to answer the three questions below.

Q1. How much communication/memory-efficient and accurate for VIRGOS? (§7.1, §7.2, §7.3)

Q2. How do different network conditions impact the running time of VIRGOS's inference and training? (§7.4)

Q3. How much efficiency has been improved by $(SM)^2$? (§7.5)

Graph Datasets. We consider three publication datasets widely adopted in GCN training: Citeseer [22], Cora [49], and Pubmed [20]. Their statistics are summarized in Table 5.

Table 5: Dataset Statistics

Dataset	Node	Edge	Feature	Class	# Train	# Test
Cora	2,708	5,429	1,433	7	140	1,000
Citeseer	3,312	4,732	3,703	6	120	1,000
Pubmed	19,717	44,338	500	3	60	1,000

Train/Test: number of samples in training/test dataset

Table 6: Communication (GB/epoch) for Training

Framework	Dataset		
	Cora	Citeseer	Pubmed
SecGNN	18.99	48.21	31.74
CoGNN	86.99	202.81	273.25
CoGNN-Opt	0.82	1.4	4.33
VIRGOS (SGD)	0.3075	0.5400	1.2567
VIRGOS (Adam)	0.3265	0.5600	1.2667

7.1 Communication of GCN

To evaluate communication costs in VIRGOS, we record the transmitting data, including frame and MPC-related data in both online and offline phases, across the servers or ports. The inference refers to a forward propagation, while the training involves an epoch of training. Unlike classical CNN training over independent data points, GCN training feeds up the whole graph (*i.e.*, 1 batch) in each training epoch, thus no benchmarking for batch sizes.

Secure Training. SecGNN [55] and CoGNN [63] are the only two open-sourced works for secure training with MPC. SecGNN [55] is the first work, meanwhile CoGNN [63] and its optimized version CoGNN-Opt are the most recent advances. Thus, we choose them as VIRGOS’s counterparts for comparison. Table 6 shows their comparison results. In general, VIRGOS uses ≤ 1.3 GB in all cases. Using SGD, VIRGOS uses 0.3075GB, 0.5400GB, and 1.2567GB for training over Cora, Citeseer, and Pubmed. With Adam, VIRGOS costs slightly higher communication due to SGD not needing $1/\sqrt{x}$. The additional costs are 6.2%, 3.7%, and 0.8% for training. These differences are related to the sparsity of data and the times of gradient update. All the cases above require less communication costs than CoGNN and SecGNN.

Secure Inference. Except for CoGNN and SecGNN, we additionally compare VIRGOS with the most recent secure inference work – OblivGNN [60] for comprehensiveness. Table 7 compares the communication costs. VIRGOS requires the lowest communication costs in all cases, reducing by $\sim 50\%$ of OblivGNN and $\sim 80\%$ of CoGNN-Opt.

7.2 Memory Usage

To avoid extra irrelevancy (*e.g.*, communication), we tested the memory usage on a single server, recording the largest observed value. Table 8 reports memory usage for training with $\Pi_{(SM)^2}$ and the standard Π_{Mult} using Beaver triple. Both protocols show acceptable results for smaller Cora and Citeseer datasets. Yet, $\Pi_{(SM)^2}$ saves 14.5%, 20.8% memory with secure SGD, and 10.5%, 18.2% memory with secure Adam.

Table 7: Communication for Inference

Framework	Dataset		
	Cora	Citeseer	Pubmed
SecGNN	1GB	1.7GB	2.5GB
CoGNN	85.63GB	201.29GB	263.59GB
CoGNN-Opt	0.5GB	0.91GB	2.02GB
OblivGNN-B	34.32GB	61.81GB	16.33GB
OblivGNN	0.29GB	0.41GB	1.65GB
VIRGOS	114MB	274MB	602MB

Table 8: Maximum Memory Usage (GB) for Training

Optimizer	Dataset	Protocol	Memory	Reduction
SGD	Cora	Beaver	1.31	
		$\Pi_{(SM)^2}$	1.12	14.5%
	Citeseer	Beaver	2.07	
		$\Pi_{(SM)^2}$	1.64	20.8%
	Pubmed	Beaver	$>28.82^{\text{M}}$	
		$\Pi_{(SM)^2}$	1.94	$>93.3\%$
Adam	Cora	Beaver	1.91	
		$\Pi_{(SM)^2}$	1.71	10.5%
	Citeseer	Beaver	2.75	
		$\Pi_{(SM)^2}$	2.25	18.2%
	Pubmed	Beaver	$>28.02^{\text{M}}$	
		$\Pi_{(SM)^2}$	2.69	$>90.4\%$

M : out-of-memory (OOM) error occurs.

The maximum memory SGD training uses is slightly lower than with Adam, as Adam’s optimization requires more memory. When training over the larger Pubmed dataset, an out-of-memory (OOM) error occurs (marked by M) when using Beaver triple, whereas the VIRGOS with $\Pi_{(SM)^2}$ supports the stable use (<2.7 GB) of memory for all datasets.

7.3 Model Accuracy

We trained the GCN over different datasets from random initialization for 300 epochs using Adam [30] with a 0.001 learning rate. Our configuration of model parameters (*i.e.*, the dimensionality of hidden layers and the number of samples) follow the original setting [31]. Since model accuracy is meaningful only for identical partitioning strategy, we compare the accuracy of secure training with plaintext in the same contexts in Table 9. Our results show that VIRGOS’s accuracy is comparable to that of plaintext training. Specifically, VIRGOS achieves {73.5%, 64.4%, 75.4%} after 100 epochs and {76.0%, 65.1%, 75.2%} after 300 epochs. Due to fluctuated training convergence, fixed-point representation, and non-linear approximation, model accuracy is slightly different.

7.4 Running Time in Different Networks

We simulate real-world deployment under different network conditions for $(SM)^2$, private inference, and private training. In particular, we consider a normal network condition (800Mbps, 0.022ms) and two poor network conditions, including a narrow-bandwidth (N.B.) network (200Mbps, 0.022ms) and high-latency (H.L.) network

Table 9: Model Accuracy

Framework	Dataset		
	Cora	Citeseer	Pubmed
Plaintext	75.7%	65.4%	74.5%
VIRGOS (100 Epochs)	73.5%	64.4%	75.4%
VIRGOS (300 Epochs)	76.0%	65.1%	75.2%

(800Mbps, 50ms). Additionally, TCP transmission involves the process of three-step handshake, data transmission, congestion control, and connection termination, thus practical time delay of $(SM)^2$ is varied below under different network conditions.

Inference Time. Table 11 compares the private inference time, including TensorFlow-Graph construction and forward-propagation computation of GCN in varying network conditions over multiple datasets. Compared to adopting Beaver triples, VIRGOS via $\Pi_{(SM)^2}$ is $\sim 7\%$ - 19% faster in the normal network, $\sim 35\%$ - 45% quicker in the narrow-bandwidth one, and saves $\sim 6\%$ - 17% time in the high-latency setting. The OOM problem prevents us from evaluating inference over Pubmed using Beaver triples, while $\Pi_{(SM)^2}$ takes ~ 30 - $50s$.

Training Time. Table 10 compares the private training time with SGD/Adam in varying network conditions over different datasets. We tested 10 epochs and got the average. In the normal network, VIRGOS via $\Pi_{(SM)^2}$ is $\sim 56\%$ - 73% faster with SGD and $\sim 42\%$ - 58% faster with Adam. In the narrow-bandwidth network, VIRGOS via $\Pi_{(SM)^2}$ is $\sim 93\%$ - 95% quicker with SGD and $\sim 84\%$ - 85% quicker with Adam. Besides, VIRGOS via $\Pi_{(SM)^2}$ is $\sim 28\%$ - 38% faster with SGD and $\sim 17\%$ - 32% faster with Adam in the high-latency setting.

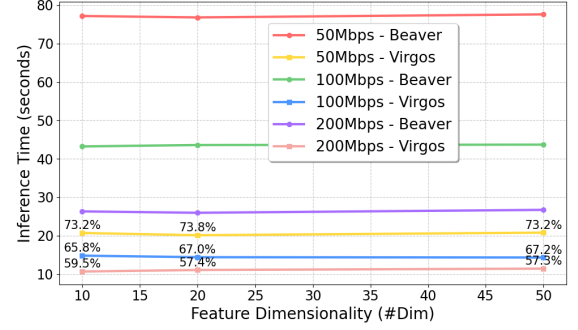
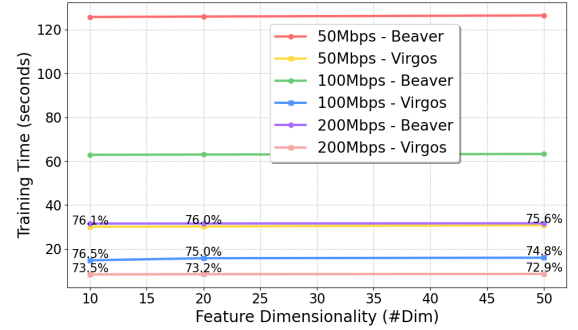
7.5 Ablation Study for $(SM)^2$

We perform extensive experiments to study the computational, communication, and memory costs saved by $(SM)^2$. Due to saving space, we defer some experimental results to Appendix A.

Communication. Table 12 reports communication comparison given varying sparsity of matrices with ~ 1000 - 5000 nodes, each with $\{1, 2, 3\}$ edges on average. In a training epoch, Beaver triples cost ~ 25 - 626 MB for sparse MM, whereas $\Pi_{(SM)^2}$ spends relatively stable costs of roughly ~ 1 - 5 MB. $\Pi_{(SM)^2}$ reduces 95% + communication compared with standard MM in all cases. At best, $\Pi_{(SM)^2}$ costs only 0.4% communication of standard one when #Node is 5000 with 1 edge on average (also the sparsest case in Table 12).

Memory Usage. Table 13 shows how sparsity affects memory usage. #Node is the total number of nodes and #Edge/Node is the average number of edges connected per node. Memory usage via Beaver triples scales with #Node, whereas $\Pi_{(SM)^2}$ maintains relatively stable use. In detail, $\Pi_{(SM)^2}$ reduces $\sim 16\%$ - 73% memory for ~ 1000 - 5000 nodes.

Running Time under Varying Network Conditions. Table 21 reports the running time of 10 epochs of $(SM)^2$ in the normal, narrow-bandwidth, and high-latency networks. In the normal network, $\Pi_{(SM)^2}$ achieves a ~ 1.1 - $26.3\times$ speed-up compared with Beaver triples. In the narrow-bandwidth network, $\Pi_{(SM)^2}$ is ~ 1.53 - $41.96\times$ faster, showing a higher speed-up than the normal network. In the

**Figure 8: Inference Time with Feature Dimensionality****Figure 9: Training Time with Feature Dimensionality**

high-latency network, $\Pi_{(SM)^2}$ shows a slightly lower speed-up than the normal network. The reason is that $\Pi_{(SM)^2}$ uses more rounds of communication than Beaver triples. It would be interesting to explore reducing round complexity for $(SM)^2$ in the future.

Running Time with Varying Dimensionality. In practice, feature dimensionality (e.g., salary, life cost) is not very high. We vary it across $\{10, 20, 50\}$ over the Citeseer dataset in Figures 8, 9 (results for other datasets are in Appendix A). We test both inference and training times. The fewer feature dimensions, the higher the percentage of costs is from SMM. Roughly, the time costs have been reduced by ~ 50 - 75% .

8 Related Works

Privacy-Preserving Machine Learning (PPML) with MPC. In the past decade, PPML has gained great attention as establishing a well-performing neural network often requires massive sensitive data, e.g., human faces, medical records. Cryptography, especially MPC, provides a handy tool to hide all inputs and intermediate results from adversaries. Secure computation of various operations [19, 32, 37, 46, 51, 56, 61, 62] like softmax and ReLU has been realized efficiently. GPU-friendly frameworks/libraries like CryptGPU [51] and Piranha [56] have been also proposed. They have shown good computational performance in training CNNs. However, most works are not tailored for GCNs, especially those computation over large and sparse structures.

Table 10: 1-Epoch Training Time (seconds) in Normal, Narrow-Bandwidth, or High-Latency Networks

Dataset	Protocol	Normal (800Mbps, 0.022ms)		N.B. (200Mbps, 0.022ms)		H.L. (800Mbps, 50ms)	
		SGD	Adam	SGD	Adam	SGD	Adam
Cora	Beaver	6.55	7.89	25.98	27.55	11.70	19.57
	$\Pi_{(SM)^2}$	4.20	5.55	13.29	14.88	9.11	16.72
	(Saving)	35.9%	29.7%	48.8%	46.0%	22.1%	14.6%
Citeseer	Beaver	11.66	13.20	46.31	48.75	18.53	27.93
	$\Pi_{(SM)^2}$	6.77	8.35	24.00	26.44	13.47	21.26
	(Saving)	41.9%	36.7%	48.2%	45.8%	27.3%	23.9%
Pubmed	Beaver	OOM	OOM	OOM	OOM	OOM	OOM
	$\Pi_{(SM)^2}$	22.87	24.45	63.69	63.58	32.00	39.86

Table 11: Inference Time (seconds) in Varying Networks

Dataset	Protocol	Normal	N.B.	H.L.
Cora	Beaver	17.48	28.34	24.22
	$\Pi_{(SM)^2}$	16.27	21.06	22.76
	(Saving)	6.9%	25.7%	6.0%
Citeseer	Beaver	24.57	44.39	33.32
	$\Pi_{(SM)^2}$	20.58	30.57	28.49
	(Saving)	16.2%	31.3%	14.5%
Pubmed	Beaver	OOM	OOM	OOM
	$\Pi_{(SM)^2}$	29.38	49.93	38.40

N.B.: narrow bandwidth, H.L.: high latency

Table 12: Communication Costs (MB) for SMM

#E/N	#Node	Beaver	$\Pi_{(SM)^2}$	Saving
1	1000	25.1	0.8	96.8%
1	2000	100.3	1.3	98.7%
1	5000	626.1	2.8	99.6%
2	1000	25.1	1.0	95.9%
2	2000	100.3	1.8	98.2%
2	5000	626.0	3.9	99.4%
3	1000	25.1	1.3	95.0%
3	2000	100.3	2.2	97.8%
3	5000	626.1	5.1	99.2%

#E/N: ratio of edges per node,

“Beaver”: using Beaver triples for SMM

Table 13: Memory Usage (MB) Given Varying Sparsity

#E/N	#Node	Beaver	$\Pi_{(SM)^2}$	Saving
1	1000	688.6	572.7	16.83%
1	2000	1236.5	575.9	53.42%
1	5000	2136.0	583.7	72.67%
2	1000	680.6	575.1	15.50%
2	2000	1173.4	579.8	50.59%
2	5000	2135.8	596.1	72.09%
3	1000	719.2	578.5	19.56%
3	2000	1142.0	582.2	49.02%
3	5000	2136.8	605.3	71.67%

Secure (Dense) Matrix Multiplication. Classical secret-sharing schemes produce secret-shares to dense matrix multiplication. Recent works [16, 26, 38, 39] designed more efficient protocols to reduce communication costs. Yet, directly adapting these to sparse structures still results in high memory/communication costs asymptotically growing with the matrix size. Large communication overhead persists as a major concern in PPML, e.g., consuming 94% of the training time of Piranha [56]. Even worse, large matrix computations are not supported due to memory overflow. So, minimizing communication costs and memory usage of $(SM)^2$ is crucial.

Standard matrix decomposition methods, such as singular value decomposition (SVD) [5] and LU decomposition (LUD) [9], are designed for faster plaintext computations rather than reducing communication in secure MPC. Thus, employing these decompositions in secure GCN does not significantly lower communication costs. Specifically, SVD decomposes a matrix into dense and diagonal matrices, while LUD decomposes it into triangular matrices. They both require $O(|V|^2)$ communication for secure multiplications in GCNs. Our decomposition approach instead adapts the graph topology into a sequence of linear transformations to exploit the sparsity, finally achieving $O(|E|)$ communication.

Sparsity Exploration in MPC. Exploiting the sparsity in plaintext can speed up the computation. Directly encoding the input sparse matrices into random matrices for acquiring privacy destroys the sparsity [59]. Several recent works [8, 59] studied the secret-shared sparse matrices and their multiplication by bridging the trade-offs between sparsity and privacy. Specifically, they relax the privacy constraint by focusing on multiplying a secret-shared matrix with a public matrix. Unlike their works, we work in the classical MPC settings, where all inputs are secretly shared. We also represent the sparsity through algebra relations (without destroying the sparsity).

ROOM [48] presents three instantiations of sparse matrix-vector multiplications optimized for different sparsity settings, such as row- and column-sparse matrices. Our decomposition works on arbitrary-sparse matrices, in contrast to either row- or column-sparse as in ROOM [48], hence eliminating the need to know the sparsity types for the input matrices. Chen *et al.* [14] realize $(SM)^2$ by sending a homomorphically encrypted dense matrix to the party holding the sparse matrix to perform ciphertext multiplication and split the result into secret shares. The limited support of homomorphic multiplication curbs this approach.

Table 14: MPC Frameworks for Secure Graph Learning

Framework	Scenario	Inference	Training	Security
OblivGNN [60]	MLaaS	✓	×	Semi-honest
LinGCN [43]	MLaaS	✓	×	Semi-honest
Penguin [45]	MLaaS	✓	×	Semi-honest
CoGNN [63]	Horizontal	✓	✓	Semi-honest
VIRGOS	Vertical	✓	✓	Semi-honest

Relevant Primitives for (SM)². Using oblivious shuffle to realize (SM)² demands $O(|V|)$ rounds of OP. We aim to hide the corresponding permutations directly in $O(1)$ rounds without using oblivious shuffle [25, 50] or sorting [2]. OLGA [4] achieves OP as a special case of linear group action. Its subsequent work [2] also uses replicated secret sharing. In VIRGOS, private permutation operation is owned by the graph holder, leading to better efficiency as in Table 2. Zou *et al.* [63] design a permutation protocol by packing the permutation-relied computation into offline to optimize the online communication. Differently, we make the offline phase independent of derived permutation, thus promisingly enabling varying graph setting (a.k.a inductive training [57]).

Another primitive of Oblivious Selection-Multiplication (OSM) is to obviously indicate whether message passing exists in an edge. Previous works like Multiplexer [46] and binary-arithmetic multiplication [19] can be adopted to realize the OSM’s functionality. Multiplexer [46], realized by two instances of 1-out-of-2 OT, requiring $2(2L + 1)$ bits. Binary-arithmetic conversion communicates $L(L + 1)/2$ bits for a 64-bit data. However, VIRGOS’s OSM protocol requires $L + 1$ bits online in 1 round using secret sharing (free of logarithm rounds of combining OT).

Secure Graph Analysis. Secure graph analysis [1, 40] can be adopted for (SM)² by reversing the graph analysis process (depicted by arrows in Figure 7). Building on garbled circuits, GraphSC [40] uses an oblivious sorting to enable secure graph computation for message-passing algorithms. Garbled circuits, while providing constant round complexity, are known for their communication and computation-intensive costs. To address this, Araki *et al.* [1] improve it by replacing sorting with shuffling in the message-passing phase and use secret-sharing-based techniques to reduce the costs of communication and computation. Recently, Graphiti [33], an advancement over GraphSC, optimizes the round complexity independently of graph size, enhancing scalability for large graphs.

In contrast to aforementioned MPC-based partitioning settings, VIRGOS adopts a practical vertical partitioning approach. VIRGOS is designed to optimize MPC protocols specifically for vertically partitioned data, incorporating novel sparsity decomposition techniques, as well as new permutation and selection multiplication protocols. These innovations allow VIRGOS to yield the optimal round complexity for (SM)² and be independent of the number of graph size, thus highlighting the potential to scale and train on massive graphs under real-world network conditions.

Cryptographic Learning over Graphs. Table 14 summarizes recent advances for cryptographic graph learning. SecGNN [55] is the first try to realize secure GCN training by integrating existing PPML advances. Efficient GCN training still remains barren nowadays.

Without the customized MPC protocol for (SM)², SecGNN suffers from high communication costs in practice. As for federated training, both vertical and horizontal partitions of distributed data are vital for practical usage. Very recently, CoGNN [63] considers a collaborative training setting where each pair of computing parties knows the sub-graphs for secure training. VIRGOS considers that one party who knows the graph but not the associated data, which is vertically partitioned.

Another branch of works [43–45, 60] adopt machine learning as a service (MLaaS) to realize secure GCN inference. Penguin [45, Table 3], as the state-of-art work, largely reduces the inference latency [27] by 5.9× over the Cora dataset [49], finally reaching 10 minutes for the inference. OblivGNN [60] recently reduces it to about 2 minutes. Unlike secure inference for MLaaS, VIRGOS made a noticeable step of secure training by reducing communication costs to 114MB in roughly 20s over the same dataset.

Many works focus on different privacy (DP) guarantees [42, 47, 58], or applying HE and private information retrieval for secure social recommendation [18]. Like some prior works, sparsity is also exploited. Their technical contributions differ vastly from ours, for we consider the MPC settings.

9 Future Works

Practical Scenarios and Graph Partitions. Our work can be extended to other federated learning settings, where a set of parties hold different types of features and sub-graphs in a general case. We observe that the general case can be formulated as partitioning node features X_i and sub-matrices A_{ij} across multiple parties $\mathcal{P}_i, \mathcal{P}_j$. To optimize the practical efficiency, each pair of parties can parallel execute VIRGOS to compute $A_{ij}X_i$ securely. In future practical applications, researchers can streamline the hybrid MPC protocols by integrating plaintext handcrafts, leveraging secure computation as a pragmatic alternative for cross-organizational collaboration.

Modular Design and Security Models. New protocols in VIRGOS are designed with a modular sense, allowing it to be instantiated with different MPC protocols. Accordingly, the security model offered by the choice of MPC protocols will be carried forward, enabling VIRGOS adapting to different settings. Besides, OP and OSM are modular protocols, which may serve as building blocks of future MPC construction. New block designs can be extended to other realizations, e.g., 2PC protocols from homomorphic encryption [36] or oblivious transfer [28, 52] or oblivious shuffle [12, 50].

Different GNN Models. Besides GCN applications, our general theorem of sparse matrix decomposition holds potential for broader adoption to further graph-structured protection in the cryptographic domain. Implementing new graph models may necessitate customized protocols to accommodate the unique operations and computations introduced by these models. Beyond GCNs, VIRGOS could facilitate the future exploration of instantiating secure graph models, e.g., GraphSage [23], GAT [53].

10 Conclusion

We propose VIRGOS, a secure 2PC framework for GCN inference and training over vertically partitioned data, a neglected MPC scenario motivated by cross-institutional business collaboration. It

is supported by our (SM)² protocol using a sparse matrix decomposition method for converting an arbitrary-sparse matrix into a sequence of linear transformations and employing 1-round MPC protocols of oblivious permutation and selection-multiplication for efficient secure evaluation of these linear transformations.

Our work provides an open-source baseline and extensive benchmarks for practical usage. Theoretical and empirical analysis demonstrate VIRGOS's superior communication and memory efficiency in private GCN computations. Hopefully, our insight could motivate further research on private graph learning.

Acknowledgments

Yu Zheng sincerely appreciates the valuable discussion, editorial helps or comments from Andes Y.L. Kei, Zhou Li, Sherman S.M. Chow, Sze Yiu Chau, and Yupeng Zhang.

References

- [1] Toshinori Araki, Jun Furukawa, Kazuma Ohara, Benny Pinkas, Hanan Rosemarin, and Hikaru Tsuchida. 2021. Secure Graph Analysis at Scale. In *CCS*. 610–629.
- [2] Gilad Asharov, Koki Hamada, Dai Ikarashi, Ryo Kikuchi, Ariel Nof, Benny Pinkas, Katsumi Takahashi, and Junichi Tomida. 2022. Efficient Secure Three-Party Sorting with Applications to Data Analysis and Heavy Hitters. In *CCS*. 125–138.
- [3] Nuttapong Attrapadung, Koki Hamada, Dai Ikarashi, Ryo Kikuchi, Takahiro Matsuda, Ibuki Mishina, Hiraku Morita, and Jacob C. N. Schuldt. 2022. Adam in Private: Secure and Fast Training of Deep Neural Networks with Adaptive Moment Estimation. *PoPETs 4* (2022), 746–767.
- [4] Nuttapong Attrapadung, Goichiro Hanaoka, Takahiro Matsuda, Hiraku Morita, Kazuma Ohara, Jacob C. N. Schuldt, Tadanori Teruya, and Kazunari Tozawa. 2021. Oblivious Linear Group Actions and Applications. In *CCS*. 630–650.
- [5] Sudipto Banerjee and Anindya Roy. 2014. *Linear algebra and matrix analysis for statistics*. CRC Press, New York.
- [6] Andrew Beaumont-Smith and Cheng-Chew Lim. 2001. Parallel Prefix Adder Design. In *Computer Arith.*. 218.
- [7] Donald Beaver. 1991. Efficient Multiparty Protocols Using Circuit Randomization. In *CRYPTO*. 420–432.
- [8] Rawad Bitar, Maximilian Egger, Antonia Wachter-Zeh, and Marvin Xhemrishi. 2024. Sparsity and Privacy in Secret Sharing: A Fundamental Trade-Off. *IEEE Trans. Inf. Forensics Secur.* 19 (2024), 5136–5150.
- [9] James R Bunch and John E Hopcroft. 1974. Triangular factorization and inversion by fast matrix multiplication. In *Mathematics of Computation*. 308–313.
- [10] Ran Canetti. 2000. Security and Composition of Multiparty Cryptographic Protocols. *J. Cryptol.* 13, 1 (2000), 143–202.
- [11] Timothy Castiglia, Yi Zhou, Shiqiang Wang, Swanand Kadhe, Nathalie Baracaldo, and Stacy Patterson. 2023. LESS-VFL: Communication-Efficient Feature Selection for Vertical Federated Learning. In *ICML*. 3757–3781.
- [12] Melissa Chase, Esha Ghosh, and Oxana Poburinnaya. 2020. Secret-Shared Shuffle. In *ASIACRYPT*. 342–372.
- [13] David Chaum, Ivan Damgard, and Jeroen van de Graaf. 1987. Multiparty Computations Ensuring Privacy of Each Party's Input and Correctness of the Result. In *CRYPTO*. 87–119.
- [14] Chaochao Chen, Jun Zhou, Li Wang, Xibin Wu, Wenjing Fang, Jin Tan, Lei Wang, Alex X. Liu, Hao Wang, and Cheng Hong. 2021. When Homomorphic Encryption Marries Secret Sharing: Secure Large-Scale Sparse Logistic Regression and Applications in Risk Control. In *KDD*. 2652–2662.
- [15] Hao Chen and Ronald Cramer. 2006. Algebraic Geometric Secret Sharing Schemes and Secure Multi-Party Computations over Small Fields. In *CRYPTO*. 521–536.
- [16] Hao Chen, Miran Kim, Ilya P. Razenshteyn, Dragos Rotaru, Yongsoo Song, and Sameer Wagh. 2020. Maliciously Secure Matrix Multiplication with Applications to Private Deep Learning. In *Asiacrypt Part III*. 31–59.
- [17] Michele Ciampi, Divya Ravi, Luisa Siniscalchi, and Hendrik Waldner. 2022. Round-Optimal Multi-party Computation with Identifiable Abort. In *EUROCRYPT*. 335–364.
- [18] Jiming Cui, Chaochao Chen, Lingjuan Lyu, Carl J. Yang, and Li Wang. 2021. Exploiting Data Sparsity in Secure Cross-Platform Social Recommendation. In *NeurIPS*. 10524–10534.
- [19] Daniel Demmler, Thomas Schneider, and Michael Zohner. 2015. ABY: A Framework for Efficient Mixed-Protocol Secure Two-Party Computation. In *NDSS*.
- [20] Franck Deroncourt and Ji Young Lee. 2017. PubMed 200k RCT: a Dataset for Sequential Sentence Classification in Medical Abstracts. In *IJCNLP*. 308–313.
- [21] Lars Folkerts, Charles Gouert, and Nektarios Georgios Tsoutsos. 2023. REDsec: Running Encrypted Discretized Neural Networks in Seconds. In *NDSS*.
- [22] C. Lee Giles, Kurt D. Bollacker, and Steve Lawrence. 1998. CiteSeer: An Automatic Citation Indexing System. In *ACM Dig. Lib.* 89–98.
- [23] William L. Hamilton, Zhitao Ying, and Jure Leskovec. 2017. Inductive Representation Learning on Large Graphs. In *NeurIPS*. 1024–1034.
- [24] David Harris. 2003. A taxonomy of parallel prefix networks. In *ACSSC*. 2213–2217.
- [25] Yanxue Jia, Shifeng Sun, Hong-Sheng Zhou, Jiajun Du, and Dawu Gu. 2022. Shuffle-based Private Set Union: Faster and More Secure. In *Usenix Security*. 2947–2964.
- [26] Xiaoqian Jiang, Miran Kim, Kristin E. Lauter, and Yongsoo Song. 2018. Secure Outsourced Matrix Computation and Application to Neural Networks. In *CCS*. 1209–1222.
- [27] Chiraag Juvekar, Vinod Vaikuntanathan, and Anantha P. Chandrakasan. 2018. GAZELLE: A Low Latency Framework for Secure Neural Network Inference. In *Usenix Security*. 1651–1669.
- [28] Marcel Keller, Emmanuela Orsini, and Peter Scholl. 2016. MASCOT: Faster Malicious Arithmetic Secure Computation with Oblivious Transfer. In *CCS*. 830–842.
- [29] Marcel Keller and Ke Sun. 2022. Secure Quantized Training for Deep Learning. In *ICML*. 10912–10938.
- [30] Diederik P. Kingma and Jimmy Ba. 2015. Adam: A Method for Stochastic Optimization. In *ICLR*.
- [31] Thomas N. Kipf and Max Welling. 2017. Semi-Supervised Classification with Graph Convolutional Networks. In *ICLR*.
- [32] B. Knott, S. Venkataraman, A.Y. Hannun, S. Sengupta, M. Ibrahim, and L.J.P. van der Maaten. 2021. CrypTen: Secure Multi-Party Computation Meets Machine Learning. In *NeurIPS*. 4961–4973.
- [33] Nishat Koti, Varsha Bhat Kukkala, Arpita Patra, and Bhavish Raj Gopal. 2024. Graphiti: Secure Graph Computation Made More Scalable. In *Proceedings of the 2024 on ACM SIGSAC Conference on Computer and Communications Security, CCS*. ACM, 4017–4031.
- [34] Yehuda Lindell. 2017. How to Simulate It - A Tutorial on the Simulation Proof Technique. In *Tutorials on the Foundations of Cryptography*. 277–346.
- [35] Yang Liu, Yan Kang, Tianyuan Zou, Yanhong Pu, Yuanqin He, Xiaozhou Ye, Ye Ouyang, Ya-Qin Zhang, and Qiang Yang. 2024. Vertical Federated Learning: Concepts, Advances, and Challenges. *IEEE Trans. Knowl. Data Eng.* 36, 7 (2024), 3615–3634.
- [36] Vadim Lyubashevsky, Chris Peikert, and Oded Regev. 2010. On Ideal Lattices and Learning with Errors over Rings. In *Annual International Conference on the Theory and Applications of Cryptographic Techniques, EUROCRYPT*, Vol. 6110. 1–23.
- [37] Payman Mohassel and Peter Rindal. 2018. ABY3: A Mixed Protocol Framework for Machine Learning. In *CCS*. 35–52.
- [38] Payman Mohassel and Yupeng Zhang. 2017. SecureML: A System for Scalable Privacy-Preserving Machine Learning. In *S&P*. 19–38.
- [39] Johannes Mono and Tim Güneysu. 2023. Implementing and Optimizing Matrix Triples with Homomorphic Encryption. In *AsiaCCS*. 29–40.
- [40] Kartik Nayak, Xiao Shaun Wang, Stratis Ioannidis, Udi Weinsberg, Nina Taft, and Elaine Shi. 2015. GraphSC: Parallel Secure Computation Made Easy. In *S&P*. 377–394.
- [41] Lucien K. L. Ng and Sherman S. M. Chow. 2021. GForce: GPU-Friendly Oblivious and Rapid Neural Network Inference. In *Usenix Security*. 2147–2164.
- [42] Shweta Patwa, Danyu Sun, Amir Gilad, Ashwin Machanavajjhala, and Sudeepa Roy. 2023. DP-PQD: Privately Detecting Per-Query Gaps In Synthetic Data Generated By Black-Box Mechanisms. *Proc. VLDB Endow.* 17, 1 (2023), 65–78.
- [43] Hongwu Peng, Ran Ran, Yukui Luo, Jiahui Zhao, Shaoyi Huang, Kiran Thorat, Tong Geng, Chenghong Wang, Xiaolin Xu, Wujie Wen, and Caiwen Ding. 2023. LinGCN: Structural Linearized Graph Convolutional Network for Homomorphically Encrypted Inference. In *NeurIPS*.
- [44] Ran Ran, Wei Wang, Quan Gang, Jieming Yin, Nuo Xu, and Wujie Wen. 2022. CryptoGCN: Fast and Scalable Homomorphically Encrypted Graph Convolutional Network Inference. In *NeurIPS*.
- [45] Ran Ran, Nuo Xu, Tao Liu, Wei Wang, Gang Quan, and Wujie Wen. 2023. Penguin: Parallel-Packed Homomorphic Encryption for Fast Graph Convolutional Network Inference. In *NeurIPS*.
- [46] Deevashwer Rathee, Mayank Rathee, Nishant Kumar, Nishanth Chandran, Divya Gupta, Aseem Rastogi, and Rahul Sharma. 2020. CryptFlow2: Practical 2-Party Secure Inference. In *CCS*. 325–342.
- [47] Sina Sajadmanesh and Daniel Gatica-Perez. 2021. Locally Private Graph Neural Networks. In *CCS*. 2130–2145.
- [48] Phillip Schoppmann, Adrià Gascón, Mariana Raykova, and Benny Pinkas. 2019. Make Some ROOM for the Zeros: Data Sparsity in Secure Distributed Machine Learning. In *CCS*. 1335–1350.
- [49] Prithviraj Sen, Galileo Namata, Mustafa Bilgic, Lise Getoor, Brian Gallagher, and Tina Eliassi-Rad. 2008. Collective Classification in Network Data. *AI Mag.* 29, 3 (2008), 93–106.
- [50] Xiangfu Song, Dong Yin, Jianli Bai, Changyu Dong, and Ee-Chien Chang. 2024. Secret-Shared Shuffle with Malicious Security. In *NDSS*.

- [51] Sijun Tan, Brian Knott, Yuan Tian, and David J. Wu. 2021. CRYPTGPU: Fast Privacy-Preserving Machine Learning on the GPU. In *S&P*. 1021–1038.
- [52] Wen-Guey Tzeng. 2002. Efficient 1-Out-n Oblivious Transfer Schemes. In *PKC*. 159–171.
- [53] Petar Velickovic, Guillem Cucurull, Arantxa Casanova, Adriana Romero, Pietro Liò, and Yoshua Bengio. 2018. Graph Attention Networks. In *International Conference on Learning Representations, ICLR*. OpenReview.net.
- [54] Ganyu Wang, Bin Gu, Qingsong Zhang, Xiang Li, Boyu Wang, and Charles X. Ling. 2023. A Unified Solution for Privacy and Communication Efficiency in Vertical Federated Learning. In *NeurIPS*.
- [55] Songlei Wang, Yifeng Zheng, and Xiaohua Jia. 2023. SecGNN: Privacy-Preserving Graph Neural Network Training and Inference as a Cloud Service. *IEEE Trans. Serv. Comput.* 16, 4 (2023), 2923–2938.
- [56] Jean-Luc Watson, Sameer Wagh, and Raluca Ada Popa. 2022. Piranha: A GPU Platform for Secure Computation. In *Usenix Security*. 827–844.
- [57] Qitian Wu, Chenxiao Yang, and Junchi Yan. 2021. Towards Open-World Feature Extrapolation: An Inductive Graph Learning Approach. In *NeurIPS*. 19435–19447.
- [58] Zonghan Wu, Shirui Pan, Fengwen Chen, Guodong Long, Chengqi Zhang, and Philip S. Yu. 2021. A Comprehensive Survey on Graph Neural Networks. In *IEEE T. Neural Net. Learn. Sys.* 4–24.
- [59] Marvin Xhemrishi, Rawad Bitar, and Antonia Wachter-Zeh. 2022. Distributed Matrix-Vector Multiplication with Sparsity and Privacy Guarantees. In *ISIT*. 1028–1033.
- [60] Zhibo Xu, Shangqi Lai, Xiaoning Liu, Alsharif Abuadbbba, Xingliang Yuan, and Xun Yi. 2024. OblivGNN: Oblivious Inference on Transductive and Inductive Graph Neural Network. In *33rd USENIX Security Symposium, USENIX Security*. USENIX Association.
- [61] Yu Zheng, Wei Song, Minxin Du, Sherman S. M. Chow, Qian Lou, Yongjun Zhao, and Xiuhua Wang. 2023. Cryptography-Inspired Federated Learning for Generative Adversarial Networks and Meta Learning. In *Advanced Data Mining and Applications - 19th International Conference, ADMA, Part II (Lecture Notes in Computer Science, Vol. 14177)*. 393–407.
- [62] Yu Zheng, Qizhi Zhang, Sherman S. M. Chow, Yuxiang Peng, Sijun Tan, Lichun Li, and Shan Yin. 2023. Secure Softmax/Sigmoid for Machine-learning Computation. In *ACSAC*. 463–476.
- [63] Zhenhua Zou, Zhuotao Liu, Jinyong Shan, Qi Li, Ke Xu, and Mingwei Xu. 2024. CoGNN: Towards Secure and Efficient Collaborative Graph Learning. In *CCS*.

A More Experimental Results

Tables 15,16,17,18,19,20 present the inference and training time with varying feature dimensionality over Cora and Pubmed datasets. The results align with our conclusion in Section 7.5.

B Proofs related to Sparsity

Definition 1 (Q-type matrix). A $(0, 1)$ -matrix M of size $m \times n$ is a Q-type matrix iff there exists a monotonically non-decreasing $f : \mathbb{Z}/m\mathbb{Z} \rightarrow \mathbb{Z}/n\mathbb{Z}$ s.t. $M[i, j] = 1$ iff $j = f(i)$.

Definition 2 (P-type matrix). A $(0, 1)$ -matrix M of size $m \times n$ is a P-type matrix iff there exists a monotonically non-decreasing $f : \mathbb{Z}/n\mathbb{Z} \rightarrow \mathbb{Z}/m\mathbb{Z}$ s.t. $M[i, j] = 1$ iff $i = f(j)$.

B.1 Proof of Theorem 1

PROOF. Suppose the sparse representation of A is $\{(i_k, j_k, \lambda_k) : k = 1, \dots, t\}$ where $k \mapsto i_k$ is monotonically non-decreasing. Then, we have $A = A'_{\text{out}} \Lambda A_{\text{in}}$, where $A'_{\text{out}} \in \mathbb{M}_{m,t}(\mathcal{R})$ is a sparse matrix represented by $\{(i_k, k, 1) : k = 1, \dots, t\}$, $\Lambda = \text{diag}(\lambda_1, \dots, \lambda_t)$, $A_{\text{in}} \in \mathbb{M}_{t,n}(\mathcal{R})$ is a sparse matrix represented by $\{(k, j_k, 1) : k = 1, \dots, t\}$. Now, A'_{out} is a P-type matrix, but A_{in} is not a Q-type matrix as A_{in} does not satisfies “ $k \mapsto j_k$ is monotonically non-decreasing”. We permute the lines of A_{in} as $A'_{\text{in}} = \{(\sigma_3^{-1}(k), j_k, 1) : k = 1, \dots, t\} = \{(k, j_{\sigma_3(k)}, 1) : k = 1, \dots, t\}$ such that $k \mapsto j_{\sigma_3(k)}$ is monotonically non-decreasing. After that, we have $A_{\text{in}} = \{(k, \sigma_3^{-1}(k), 1) : k = 1, \dots, t\} \times A'_{\text{in}} = \{(\sigma_3(k), k, 1) : k = 1, \dots, t\} \times A'_{\text{in}} = \sigma_3 A'_{\text{in}}$, where A'_{in} is a Q-type matrix. Hence, $A = A'_{\text{out}} \Lambda \sigma_3 A'_{\text{in}}$. \square

B.2 Proof of Theorem 2

PROOF. The proof is straightforward by composing $A = A'_{\text{out}} \Lambda \sigma_3 A'_{\text{in}}$ from Theorem 1, $A'_{\text{in}} = \Sigma \sigma_2 \Gamma_{\text{in}} \delta_n \sigma_1$ from Theorem 4, and $A'_{\text{out}} = \sigma_5 \delta_m^T \Gamma_{\text{out}} \sigma_4 \Sigma^T$ from Theorem 5. \square

B.3 Proof of Theorem 3

PROOF. It is straightforward to prove by observing that:

- 1) Permutations on σ_i calls permutation group action;
- 2) Multiplying δ, Σ calls constant matrix multiplication;
- 3) Multiplying $\Gamma_{\text{in}}, \Gamma_{\text{out}}$ calls element-wise multiplication (with cut-off and padding of zero values);
- 4) Multiplying Λ calls element-wise multiplication. \square

B.4 Proof of Theorem 4

THEOREM 4. Let $A'_{\text{in}} \in \mathbb{M}_{t,n}$ be a Q-type matrix with n_{col} non-zero columns. Then, there exists a matrix decomposition $A'_{\text{in}} = \Sigma \sigma_2 \Gamma_{\text{in}} \delta_n \sigma_1$ where $\sigma_1 \in \mathbb{S}_n, \sigma_2 \in \mathbb{S}_t$, and,

- 1) $\Sigma = (\Sigma[i, j])_{i,j=1}^t$ is the left-down triangle matrix such that $\Sigma[i, j] = 1$ if $i \geq j$ or 0 otherwise,
- 2) $\delta_n = (\delta_n[i, j])_{i,j=1}^n$ is the left-down triangle matrix such that $\delta_n[i, j] = 1$ for $i = j$ or -1 for $j = i - 1$, or 0 otherwise,
- 3) $\Gamma_{\text{in}} = (\Gamma_{\text{in}}[i, j])_{i=1,j=1}^{t,n}$ is a matrix such that $\Gamma_{\text{in}}[i, j] = 1$ for $1 \leq i = j \leq n_{\text{col}}$ or 0 otherwise.

PROOF. Here, we prove that $A'_{\text{in}} X = \Sigma \sigma_2 \Gamma_{\text{in}} \delta_n \sigma_1 X$ holds for any $X \in \mathcal{R}^{(n)}$. Firstly, we can use column transformation to transform matrix A'_{in} to a new matrix \tilde{A}'_{in} of Q-type such that all the $n - n_{\text{col}}$ zero-columns of \tilde{A}'_{in} lie in the last columns. Hence, we have $A'_{\text{in}} = \tilde{A}'_{\text{in}} \sigma_1$, and \tilde{A}'_{in} is in the form of,

$$A'_{\text{in}} = \begin{pmatrix} 1 & & 0 & \cdots & 0 \\ \vdots & & & & \\ \vdots & & & & \\ 1 & & \vdots & & \vdots \\ & 1 & & & \\ \vdots & & \vdots & & \vdots \\ 1 & & \vdots & & \vdots \\ & & \ddots & & \vdots \\ & & & 1 & \\ & & & \vdots & \\ & & & 1 & 0 & \cdots & 0 \end{pmatrix}$$

Table 15: Inference Time (seconds) with Varying Feature Dimensionality over Cora

#Dim	50Mbps			100Mbps			200Mbps		
	Beaver	$\Pi_{(SM)^2}$	Saving	Beaver	$\Pi_{(SM)^2}$	Saving	Beaver	$\Pi_{(SM)^2}$	Saving
1433	64.18	33.53	47.8%	35.99	20.74	42.4%	22.03	14.62	33.6%
10	51.96	19.55	62.4%	29.56	14.33	51.5%	18.89	10.80	42.8%
20	52.59	19.06	63.8%	30.25	13.86	54.2%	18.48	10.62	42.5%
50	52.04	19.42	62.7%	29.71	13.96	53.0%	18.69	11.38	39.1%

#E/N: ratio of edges per node, "Beaver": using Beaver triples for MM.

Table 16: Inference Time (seconds) with Varying Feature Dimensionality over Citeseer

#Dim	50Mbps			100Mbps			200Mbps		
	Beaver	$\Pi_{(SM)^2}$	Saving	Beaver	$\Pi_{(SM)^2}$	Saving	Beaver	$\Pi_{(SM)^2}$	Saving
3703	117.83	62.36	47.1%	64.04	35.78	44.1%	37.36	23.29	37.7%
10	77.18	20.69	73.2%	43.22	14.79	65.8%	26.31	10.66	59.5%
20	76.81	20.11	73.8%	43.59	14.39	67.0%	25.95	11.06	57.4%
50	77.60	20.78	73.2%	43.69	14.31	67.2%	26.71	11.41	57.3%

Table 17: Inference Time (seconds) over Pubmed

#Dim	50Mbps		100Mbps		200Mbps	
	Beaver	$\Pi_{(SM)^2}$	Beaver	$\Pi_{(SM)^2}$	Beaver	$\Pi_{(SM)^2}$
500	OOM	132.06	OOM	69.66	OOM	42.37
10	OOM	92.70	OOM	53.35	OOM	32.77
20	OOM	92.94	OOM	53.88	OOM	34.22
50	OOM	93.87	OOM	54.67	OOM	33.49

Let $\tilde{X} = \sigma_1 X$, then we have $A'_{in} \tilde{X}$ equal to:

$$A'_{in} \tilde{X} = \begin{pmatrix} \tilde{x}_1 \\ \tilde{x}_1 \\ \vdots \\ \tilde{x}_1 \\ \tilde{x}_2 \\ \tilde{x}_2 \\ \vdots \\ \tilde{x}_2 \\ \vdots \\ \vdots \\ \tilde{x}_{n_{col}} \\ \tilde{x}_{n_{col}} \\ \vdots \\ \tilde{x}_{n_{col}} \end{pmatrix} = \Sigma \begin{pmatrix} \tilde{x}_1 \\ 0 \\ \vdots \\ 0 \\ \tilde{x}_2 - \tilde{x}_1 \\ 0 \\ \vdots \\ 0 \\ \vdots \\ \vdots \\ \tilde{x}_{n_{col}} - \tilde{x}_{n_{col}-1} \\ 0 \\ \vdots \\ 0 \end{pmatrix}$$

$$= \Sigma \sigma_2 \begin{pmatrix} \tilde{x}_1 \\ \tilde{x}_2 - \tilde{x}_1 \\ \vdots \\ \tilde{x}_{n_{col}} - \tilde{x}_{n_{col}-1} \\ 0 \\ \vdots \\ 0 \end{pmatrix} = \Sigma \sigma_2 \Gamma_{in} \begin{pmatrix} \tilde{x}_1 \\ \tilde{x}_2 - \tilde{x}_1 \\ \vdots \\ \tilde{x}_{n_{col}} - \tilde{x}_{n_{col}-1} \\ \tilde{x}_{n_{col}+1} - \tilde{x}_{n_{col}} \\ \vdots \\ \tilde{x}_n - \tilde{x}_{n-1} \end{pmatrix}$$

$$= \Sigma \sigma_2 \Gamma_{in} \delta_n \tilde{X} = \Sigma \sigma_2 \Gamma_{in} \delta_n \sigma_1 X. \quad \square$$

B.5 Proof of Theorem 5

THEOREM 5. Let $A'_{out} \in \mathbb{M}_{m,t}(\mathcal{R})$ be a P-type matrix with n_{row} non-zero rows. Then, there exists a matrix decomposition $A'_{out} = \sigma_5 \delta_m^T \Gamma_{out} \sigma_4 \Sigma^T$ where $\sigma_5 \in \mathbb{S}_m$, $\sigma_4 \in \mathbb{S}_t$, and,

- 1) $\Sigma = (\Sigma[i, j])_{i,j=1}^t$ is the left-down triangle matrix such that $\Sigma[i, j] = 1$ if $i \geq j$ or 0 otherwise,
- 2) $\delta_m = (\delta_m[i, j])_{i,j=1}^m$ is the left-down triangle matrix such that $\delta_m[i, j] = 1$ for $i = j$ or -1 for $j = i - 1$, or 0 otherwise,
- 3) $\Gamma_{out} = (\Gamma_{out}[i, j])_{i=1,j=1}^{m,t}$ is a matrix such that $\Gamma_{out}[i, j] = 1$ for $1 \leq i = j \leq n_{row}$ or 0 otherwise.

PROOF. Note that $(A'_{out})^T \in \mathbb{M}_{t,m}$ is a Q-type matrix, we have the matrix decomposition $(A'_{out})^T = \Sigma \sigma_2 \Gamma_{in} \delta_m \sigma_1$ by Theorem 4, where $\sigma_1 \in \mathbb{S}_m$ and $\sigma_2 \in \mathbb{S}_t$. Let $\sigma_5 = \sigma_1^T$, $\sigma_4 = \sigma_2^T$, $\Gamma_{out} = \Gamma_{in}^T$, we have $A'_{out} = \sigma_5 \delta_m^T \Gamma_{out} \sigma_4 \Sigma^T$. \square

C Algorithm Realization

Guided by Theorem 1, our algorithm of decomposing the adjacency matrix A can be implemented as below. A is a SparseMatrix consists of all 0-1 elements represented by coordinates of nonzero values, i.e., [(row-index, column-index), (row-index, column-index), ...]. In Figure 10, we draw the pairs of (row-index, column-index) of A, e.g., [(2, 3), (3, 1), ...]. Step 1 is to split the pairs in A to construct two sparse matrices (Graph language in Figure 2b), called P' and Q' (correspond to A_{out} and A_{in} in Section 4.1). In Steps 2 and 3,

Table 18: Training Time (seconds) with Varying Feature Dimensionality over Cora

#Dim	50Mbps			100Mbps			200Mbps		
	Beaver	$\Pi_{(SM)^2}$	Saving	Beaver	$\Pi_{(SM)^2}$	Saving	Beaver	$\Pi_{(SM)^2}$	Saving
1433	106.31	50.50	52.5%	53.19	25.79	51.5%	22.03	13.58	38.4%
10	86.05	29.75	65.4%	43.05	15.62	63.7%	18.89	8.42	55.4%
20	86.18	29.89	65.3%	43.13	15.47	64.1%	18.48	8.48	54.1%
50	86.62	30.30	65.0%	43.34	15.77	63.6%	18.69	8.65	53.7%

Table 19: Training Time (seconds) with Varying Feature Dimensionality over Citeseer

#Dim	50Mbps			100Mbps			200Mbps		
	Beaver	$\Pi_{(SM)^2}$	Saving	Beaver	$\Pi_{(SM)^2}$	Saving	Beaver	$\Pi_{(SM)^2}$	Saving
3703	190.04	94.60	50.2%	95.06	47.86	49.7%	47.65	24.58	48.4%
10	125.78	30.08	76.1%	62.91	14.79	76.5%	31.54	8.35	73.5%
20	125.97	30.23	76.0%	63.03	15.75	75.0%	31.57	8.46	73.2%
50	126.47	30.83	75.6%	63.29	15.98	74.8%	31.68	8.58	72.9%

Table 20: Training Time (seconds) over Pubmed

#Dim	50Mbps		100Mbps		200Mbps	
	Beaver	$\Pi_{(SM)^2}$	Beaver	$\Pi_{(SM)^2}$	Beaver	$\Pi_{(SM)^2}$
500	OOM	233.53	OOM	118.23	OOM	64.16
10	OOM	175.14	OOM	92.90	OOM	51.27
20	OOM	176.75	OOM	92.52	OOM	51.72
50	OOM	180.08	OOM	93.53	OOM	52.71

#E/N: edges per node ratio, "Beaver": Beaver triples for MM

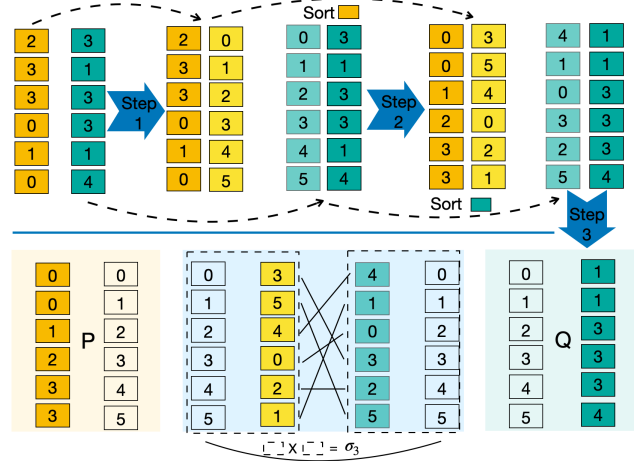
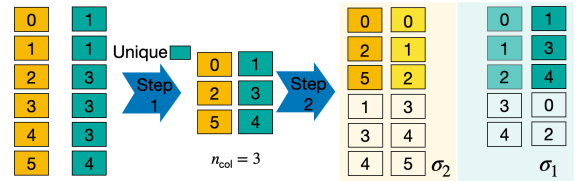
the row-indices of P' are sorted and generate σ_3^P , and the column-indices of Q' are sorted and generate σ_3^Q . Then, σ_3 is obtained by sparse-matrix multiplying σ_3^P and σ_3^Q , thus $\sigma_3 = \sigma_3^P \cdot \sigma_3^Q$. Now, we can see that the resulting matrices P and Q (correspond to A'_{out} and A'_{in} in Section 4.2) have monotonically non-decreasing row/column indices. Moreover, P contain exactly one 1 in every column and Q contains exactly one 1 in every row. In summary, the pseudocode of `decompose_row_column(A)` below describes the extraction of P , σ_3 and Q as previously displayed in Figure 4.

```
def decompose_row_column(A):
```

```
#A: a list of (row_id, col_id) for non-zero element in sparse matrix
```

```
P=[(A[i, 0], i) for i in range(len(A))]
Q=[(i, A[i, 1]) for i in range(len(A))]
P=sorted(P, key=lambda x: x[0])
Q=sorted(Q, key=lambda x: x[1])
P=[(P[i,0], i) for i in range(len(A))]
sigma3P=[(i, P[i,1]) for i in range(len(A))]
sigma3Q=[(Q[i,0], i) for i in range(len(A))]
Q=[(i,Q[i,1]) for i in range(len(A))]
sigma3 = sigma3P*sigma3Q
return P, sigma3, Q
```

Pseudocode of re-decomposition. In Figure 11, we re-draw Q and describe its decomposition. Step 1 extracts the unique column indices using set function in Python, and their quantity is n_{col} . Then, the corresponding row indices are extracted by comparing whether the neighboring column indices are identical. Step 2 constructs σ_1

**Figure 10: Illustration of $P\sigma_3Q$ Decomposition****Figure 11: Illustration of Q Decomposition**

and σ_2 by keeping the first n_{col} elements and padding the elements in numerical order to a permutation in $\sigma_1 \in \mathbb{S}_n, \sigma_2 \in \mathbb{S}_t$. The code of decomposing Q is outlined below. To derive σ_4, n_{row} , and σ_5 , the P -type matrix decomposition follows a similar logic.

```
def decompose_Q(Q, e, n):
```

```
unique_col_ids = set(Q[:,1])
step_row_ids=[Q[i,0] for Q[i, 1]!=Q[i-1, 1] or i=0]
k2 = len(unique_col_ids)
sigma1 = [ (i, unique_col_ids[i] ) for i in range(k2)]
```


Table 21: 10-Epoch Running Time (seconds) of $(SM)^2$ in Varying Networks

#E/N	#Node	Normal (800Mbps, 0.022ms)			N.B. (200Mbps, 0.022ms)			H.L. (800Mbps, 50ms)		
		Beaver	$(SM)^2$	Saving	Beaver	$(SM)^2$	Saving	Beaver	$(SM)^2$	Saving
1	1000	3.79	2.92	23.0%	8.89	3.07	65.5%	7.55	8.57	11.9%
1	3000	60.67	4.70	92.3%	106.39	5.15	95.2%	74.54	10.00	86.6%
1	5000	165.35	6.30	96.2%	294.11	7.01	97.6%	203.77	11.53	94.3%
2	1000	5.95	5.54	6.9%	10.92	5.72	47.6%	9.17	10.88	–
2	3000	62.48	7.99	87.2%	108.42	8.57	92.1%	76.64	13.24	82.7%
2	5000	168.06	10.57	93.7%	296.50	11.71	96.1%	206.38	15.82	92.3%
3	1000	8.27	8.62	4.2%	13.61	8.89	34.7%	11.83	13.93	–
3	3000	64.45	11.92	81.5%	111.71	12.74	88.6%	79.58	17.19	78.4%
3	5000	170.01	15.28	91.0%	299.57	16.77	94.4%	209.03	20.64	90.1%

#E/N: ratio of edges per node, “Beaver”: using Beaver triples

```
sigma2 = [(step_row_ids[i], i) for i in range(k2)]
sigma1=pad_perm(sigma1, n)
sigma2=pad_perm(sigma2, e)
return sigma2, k2, sigma1
```

The class `PrivateSparseMatrix` below contains the realization of $(SM)^2$ protocols. Before secure training, the graph owner locally decomposes A into P, Q , and then into the corresponding basic operations. $(SM)^2$ let \mathcal{P}_0 and \mathcal{P}_1 jointly execute secure multiplications on P and Q , and OP on σ_3 .

```
class PrivateSparseMatrix:
```

```
def __init__(self, A ...):
    self.owner = get_device()
    with tf.device(self.owner):
        P, s3, Q = decompose_row_column()
        s5, k4, s4 = decompose_P()
        s2, k2, s1 = decompose_Q()
def sm_2(self, x: Union[PrivateTensor,
    SharedPair]):
    Qx = Q_mult(s2, k2, s1, e, x)
    x3 = s3.act(Qx)
    Ax = P_mult(s5, k4, s4, x3, m)
    return Ax
```

Class of Secure GCN. The implementation of VIRGOS follows the plaintext-training repository (<https://github.com/dmlc/dgl>) in the transductive setting. Accordingly, the graph decomposition can be performed once with the fixed graph before secure training. The class `SGCN` inherits the conventional NN (the template of neural network). Secure GCN training is thus composed of secure graph convolution and secure activation layers. The AX in graph convolution layers is realized by the $\Pi_{(SM)^2}$ protocol. Below, we extract the code of implementing the class `SGCN` with respect to the plaintext GCN. Notably, all the inputs `feature`, `label`, and `adj_matrix` are secret shares in the form of fixed-pointed numbers. The functions `GraphConv`, `ReLU`, `SoftmaxCE` are the MPC protocols executed by two parties.

```
class SGCN(NN):
```

```
def __init__(self, feature: PrivateTensor,
    label: PrivateTensor,
    dense_dims: List[int],
    adj_matrix: Union[...],
```

```
    train_mask, loss=...):
    super(SGCN, self).__init__()
    layer = Input(dim, feature)
    self.addLayer(layer)
    input_layers = [layer]
    for i in range(1, len(dense_dims)):
        layer = GraphConv()
        self.addLayer(layer)
        if i < len(dense_dims) - 1:
            layer = ReLU()
            self.addLayer(layer)
    layer_label = Input(dim, label)
    self.addLayer(layer_label)
    if loss == "SoftmaxCE":
        layer_loss = SoftmaxCE()
        self.addLayer(layer_loss)
    else:
        ...# use other layer/loss
```

D Selection-Multiplication’s Correctness

PROOF OF LEMMA 1. We analyze the two cases of $s = 0$ and $s = 1$ for a complete proof where $s \in \{0, 1\}$.

(i). When $s = 0$, the equivalence of the first property turns to be $f(0, x + u) = f(0, x) + f(0, u) \Leftrightarrow 0 \cdot (x + u) = 0 \cdot x + 0 \cdot u \Leftrightarrow 0 = 0$. When $s = 1$, we have $f(1, x + u) = f(1, x) + f(1, u) \Leftrightarrow 1 \cdot (x + u) = 1 \cdot x + 1 \cdot u \Leftrightarrow x + u = x + u$.

(ii). When $s = 0$, the second property becomes $f(0 + b, x) = f(0, x) + (-1)^0 f(b, x) \Leftrightarrow bx = 0 \cdot x + 1 \cdot bx \Leftrightarrow bx = bx$. When $s = 1$, we have $f(1 + b, x) = f(1, x) + (-1)^1 f(b, x) \Leftrightarrow (1 + b) \cdot x = 1 \cdot x - bx$. If $b = 0$, we get $x = x$. If $b = 1$, we get $0 = 0$ since $(1 + b) \bmod 2 = 0$. \square

E Security Analysis

We prove the semi-honest security of our protocols under the real/ideal-world simulation paradigm [34] with a hybrid argument. As our protocols satisfy the stand-alone model without malicious assumption, we adopt the standard simulation proof technique instead of the UC framework that adds an additional “environment” representing an interactive distinguisher.

We consider the 2PC executed by \mathcal{P}_0 and \mathcal{P}_1 in the presence of static semi-honest adversaries \mathcal{A} that control one of the parties at the beginning, follow the protocol specification, and try to learn

Functionality 1 \mathcal{F}_{OP} : Ideal Functionality of Π_{OP} **Parameter:** Type of input type $\in \{\text{plain, shared}\}$.**Input:** $\sigma \in \mathbb{S}, X \in \mathbb{Z}^m$ if type == plain;
otherwise $\sigma \in \mathbb{S}, \langle X \rangle_0 \in \mathbb{Z}^m, \langle X \rangle_1 \in \mathbb{Z}^m$.**Output:** $\langle \sigma X \rangle_0, \langle \sigma X \rangle_1$.

- 1: **if** type == shared **then**
- 2: Reconstruct $X = \langle X \rangle_0 + \langle X \rangle_1$
- 3: **end if**
- 4: Compute and generate random shares of σX
- 5: **return** $\langle \sigma X \rangle$

information about the honest party's private input. Definition 3 states the semi-honest security so that simulated and real execution are computationally indistinguishable (" \equiv ") for \mathcal{A} . That is, the simulator \mathcal{S} can generate the view of a party in the execution, implying the party learns nothing beyond what they can derive from their input and prescribed output. For simplicity, we assume PRF to be secure and exclude its standard proof here.

Definition 3 (Semi-honest Security [34]). *Let λ be a security parameter. A protocol Π securely realizes a functionality $\mathcal{F} = (\mathcal{F}_0, \mathcal{F}_1)$ on input $\langle x \rangle = (\langle x \rangle_0, \langle x \rangle_1)$ against static semi-honest adversaries if there exist PPT simulators $\mathcal{S}_0, \mathcal{S}_1$ s.t.*

$$\{\mathcal{S}_0(1^\lambda, \langle x \rangle_0, \mathcal{F}_0), \mathcal{F}(\langle x \rangle)\} \equiv \{\text{view}_0^\Pi, \text{output}^{\Pi, \lambda}(\langle x \rangle)\},$$

$$\{\mathcal{S}_1(1^\lambda, \langle x \rangle_1, \mathcal{F}_1), \mathcal{F}(\langle x \rangle)\} \equiv \{\text{view}_1^\Pi, \text{output}^{\Pi, \lambda}(\langle x \rangle)\}.$$

E.1 Security of Π_{OP}

We divide the analyses into 'raw' and 'shared' cases. Functionality 1 presents the ideal functionality \mathcal{F}_{OP} . It contains two cases in which the input vector/matrix X is owned by one party or secret-shared among two parties. The functionality \mathcal{F}_{OP} of both cases outputs additive shares of permutation over X , i.e., $\langle \sigma X \rangle_0 + \langle \sigma X \rangle_1 = \sigma X$.

THEOREM 6. *The protocol Π_{OP} securely realizes the ideal functionality \mathcal{F}_{OP} against static semi-honest adversaries.*

PROOF. We define the following Ideal and Real experiments:

$$\text{Real}_{\Pi_{\text{OP}}}^{1^\lambda, \mathcal{A}} = \{ \{ (\text{view}_0^{\Pi, \text{plain}}, \langle \sigma X \rangle_0), (\text{view}_1^{\Pi, \text{plain}}, \langle \sigma X \rangle_1) \} \text{ or} \\ \{ (\text{view}_0^{\Pi, \text{shared}}, \langle \sigma X \rangle_0), (\text{view}_1^{\Pi, \text{shared}}, \langle \sigma X \rangle_1) \} \}$$

$$\text{Ideal}_{\mathcal{S}, \mathcal{F}}^{1^\lambda, \mathcal{A}} = \{ \{ \mathcal{S}(\text{plain}, 1^\lambda, \sigma, X, \mathcal{F}_{\text{OP}}), \mathcal{F}_{\text{OP}}(\sigma, X) \} \text{ or} \\ \{ \mathcal{S}(\text{shared}, 1^\lambda, \sigma, \langle X \rangle_0, \langle X \rangle_1, \mathcal{F}_{\text{OP}}), \\ \mathcal{F}_{\text{OP}}(\sigma, \langle X \rangle_0, \langle X \rangle_1) \} \}$$

where \mathcal{P}_0 's view is either $\text{view}_0^{\Pi, \text{plain}}$, which is $(\sigma, \pi, \langle \pi U \rangle_0, \delta_\sigma, \delta_X)$ or $\text{view}_0^{\Pi, \text{shared}}$, which is $(\sigma, \langle X \rangle_0, \pi, \langle \pi U \rangle_0, \delta_\sigma, \delta_{\langle X \rangle_1})$, and \mathcal{P}_1 's view is either $\text{view}_1^{\Pi, \text{plain}} = (X, \langle \pi U \rangle_1, \delta_\sigma, \delta_X)$ or $\text{view}_1^{\Pi, \text{shared}} = (\langle X \rangle_1, \langle \pi U \rangle_1, \delta_\sigma, \delta_{\langle X \rangle_1})$. $\text{Real}_{\Pi_{\text{OP}}}^{1^\lambda, \mathcal{A}}$ represents real protocol execution. In the Ideal world, the simulators $\mathcal{S} = \{\mathcal{S}_0, \mathcal{S}_1\}$ can indistinguishably simulate the view of each honest party in the protocol given only that party's input.

Now, we argue that $\text{Real}_{\Pi_{\text{OP}}}^{1^\lambda, \mathcal{A}} \equiv \text{Ideal}_{\mathcal{S}, \mathcal{F}}^{1^\lambda, \mathcal{A}}$ for any PPT \mathcal{A} using the multi-step hybrid-argument technique.

Functionality 2 \mathcal{F}_{OSM} : Ideal Functionality of Π_{OSM} **Input:** $s \in \mathbb{Z}_2, \langle x \rangle_0 \in \mathbb{Z}_2^n, \langle x \rangle_1 \in \mathbb{Z}_2^n$.**Output:** $\langle sx \rangle_0, \langle sx \rangle_1$.

- 1: Reconstruct $s = \langle s \rangle_0 + \langle s \rangle_1$
- 2: Compute and generate random shares of sx
- 3: **return** $\langle sx \rangle$

Hyb₀: It is identical to the real protocol execution $\text{Real}_{\Pi_{\text{OP}}}^{1^\lambda, \mathcal{A}}$.

Hyb₁: It is identical to **Hyb₀** except that δ_σ, δ_X are randomly generated for the case of plain and $\delta_\sigma, \delta_{\langle X \rangle_1}$ are randomly generated for the case of shared.

i) In the first case that X 's type is plain, any PPT \mathcal{A} cannot distinguish δ_σ, δ_X in $\text{Real}_{\Pi_{\text{OP}}}^{1^\lambda, \mathcal{A}}$ experiment and $\tilde{\delta}_\sigma, \tilde{\delta}_X$ in **Hyb₁** since δ_σ, δ_X are computed by π, U , which are generated by PRF. If \mathcal{A} can distinguish **Hyb₁** and $\text{Real}_{\Pi_{\text{OP}}}^{1^\lambda, \mathcal{A}}$ with non-negligible advantage, \mathcal{A} can break the security of PRF, which contradicts the assumption.

ii) For the second case that X 's type is shared, any PPT \mathcal{A} cannot distinguish $\delta_\sigma, \delta_{\langle X \rangle_1}$ in $\text{Real}_{\Pi_{\text{OP}}}^{1^\lambda, \mathcal{A}}$ experiment and $\tilde{\delta}_\sigma, \tilde{\delta}_{\langle X \rangle_1}$ in **Hyb₁** since $\delta_\sigma, \delta_{\langle X \rangle_1}$ are computed by π, U , which are generated by PRF. If \mathcal{A} can distinguish **Hyb₁** and $\text{Real}_{\Pi_{\text{OP}}}^{1^\lambda, \mathcal{A}}$ with non-negligible advantage, \mathcal{A} can break the PRF security, contradicting the assumption.

$\Rightarrow \text{Hyb}_1 \equiv \text{Hyb}_0$.

Hyb₂: It is identical to $\text{Ideal}_{\mathcal{S}, \mathcal{F}}^{1^\lambda, \mathcal{A}}$, i.e., all $\text{view}_0, \text{view}_1$ of two parties are simulated by $\mathcal{S}_0, \mathcal{S}_1$. The randomness of $\pi, \langle \pi U \rangle_0, \delta_\sigma, \delta_X$ for plain and $\pi, \langle \pi U \rangle_0, \delta_\sigma, \delta_{\langle X \rangle_1}$ for shared ensures no non-negligible \mathcal{A} 's advantage of distinguishability to \mathcal{S}_0 's view. Similarly, the randomness of $\langle \pi U \rangle_1, \delta_\sigma, \delta_X$ for plain and $\langle \pi U \rangle_1, \delta_\sigma, \delta_{\langle X \rangle_1}$ for shared ensures no non-negligible \mathcal{A} 's advantage of distinguishability to \mathcal{S}_1 's view. Now, \mathcal{P}_0 cannot obtain \mathcal{S}_1 inputs, while \mathcal{P}_1 cannot obtain \mathcal{P}_0 inputs since $\{\mathcal{S}_i\}_{i \in \{0,1\}}$ cannot obtain $\{\mathcal{S}_{1-i}\}_{i \in \{0,1\}}$'s inputs using the $\{\text{view}_i\}_{i \in \{0,1\}}$.

$\Rightarrow \text{Hyb}_2 \equiv \text{Hyb}_1$.

Thus, for both cases, we have $\text{Hyb}_2 \equiv \text{Hyb}_1 \equiv \text{Hyb}_0$, equivalent to $\text{Real}_{\Pi_{\text{OP}}}^{1^\lambda, \mathcal{A}} \equiv \text{Ideal}_{\mathcal{S}, \mathcal{F}}^{1^\lambda, \mathcal{A}}$ for any PPT semi-honest \mathcal{A} . \square

E.2 Security of Π_{OSM}

Functionality 2 gives the ideal functionality of Π_{OSM} , defining the multiplication $sx \in \mathbb{Z}_2^n$ between $s \in \mathbb{Z}_2$ and $x \in \mathbb{Z}_2^n$.

THEOREM 7. *The protocol Π_{OSM} securely realizes the ideal functionality \mathcal{F}_{OSM} against static semi-honest adversaries.*

PROOF. We define the Ideal and Real experiments:

$$\text{Real}_{\Pi_{\text{OSM}}}^{1^\lambda, \mathcal{A}} = \{ (\text{view}_0^\Pi, \langle sx \rangle_0), (\text{view}_1^\Pi, \langle sx \rangle_1) \}$$

$$\text{Ideal}_{\mathcal{S}, \mathcal{F}}^{1^\lambda, \mathcal{A}} = \{ \mathcal{S}(1^\lambda, s, \langle x \rangle_0, \langle x \rangle_1, \mathcal{F}_{\text{OSM}}), \\ \mathcal{F}_{\text{OSM}}(s, \langle x \rangle_0, \langle x \rangle_1) \}$$

Functionality 3 $\mathcal{F}_{(\text{SM})^2}$: Ideal Functionality of $\Pi_{(\text{SM})^2}$ **Input:** $A \in \mathbb{M}_{m,n}(\mathcal{R}), X \in \mathbb{M}_{n,d}(\mathcal{R})$.**Output:** $\langle AX \rangle_0, \langle AX \rangle_1$.

- 1: Compute and generate random shares of AX
- 2: **return** $\langle AX \rangle$

where $\text{view}_0^\Pi = (s, \langle x \rangle_0, b, \langle u \rangle_0, \langle bu \rangle_0, \delta_s, \delta_{\langle x \rangle_0}, \delta_{\langle x \rangle_1}, \delta_x)$, and $\text{view}_1^\Pi = (\langle x \rangle_1, \langle bu \rangle_1, \langle u \rangle_1, \delta_{\langle x \rangle_1}, \delta_s)$. $\text{Real}_{\Pi_{\text{OSM}}}^{1^\lambda, \mathcal{A}}$ represents real protocol execution. The simulators $\mathcal{S} = \{\mathcal{S}_0, \mathcal{S}_1\}$ are indistinguishably simulating the view of each honest party in the protocol given only that party's input.

Now, we prove that $\text{Real}_{\Pi_{\text{OSM}}}^{1^\lambda, \mathcal{A}} \equiv \text{Ideal}_{\mathcal{S}, \mathcal{F}}^{1^\lambda, \mathcal{A}}$ for any PPT \mathcal{A} with a series of hybrid-arguments. The hybrid games can be sequentially formulated as follows.

Hyb₀: It is identical to the real protocol execution $\text{Real}_{\Pi_{\text{OSM}}}^{1^\lambda, \mathcal{A}}$.

Hyb₁: It is identical to Hyb₀ except that $\delta_{\langle x \rangle_0}, \delta_{\langle x \rangle_1}, \delta_x$ are randomly generated by \mathcal{S}_0 . Since $\delta_{\langle x \rangle_0}, \delta_{\langle x \rangle_1}$ in $\text{Real}_{\Pi_{\text{OSM}}}^{1^\lambda, \mathcal{A}}$ experiment are computed by $\langle u \rangle_0, \langle u \rangle_1$, which are outputted by PRF. Thus, any PPT \mathcal{A} cannot distinguish $\delta_{\langle x \rangle_0}, \delta_{\langle x \rangle_1}$ in $\text{Real}_{\Pi_{\text{OSM}}}^{1^\lambda, \mathcal{A}}$ experiment and $\tilde{\delta}_{\langle x \rangle_0}, \tilde{\delta}_{\langle x \rangle_1}$ in Hyb₁, guaranteed by PRF's security. The value of δ_x , added by $\delta_{\langle x \rangle_0}$ and $\delta_{\langle x \rangle_1}$, is also distinguishable to $\tilde{\delta}_x$ simulated by \mathcal{S}_0 . Overall, if \mathcal{A} can distinguish $\tilde{\delta}_{\langle x \rangle_0}, \tilde{\delta}_{\langle x \rangle_1}, \tilde{\delta}_x$ with $\delta_{\langle x \rangle_0}, \delta_{\langle x \rangle_1}, \delta_x$ in $\text{Real}_{\Pi_{\text{OSM}}}^{1^\lambda, \mathcal{A}}$ with non-negligible advantage, \mathcal{A} can break the security of PRF.

$\Rightarrow \text{Hyb}_1 \equiv \text{Hyb}_0$.

Hyb₂: It is identical to Hyb₁ except that δ_s are randomly generated. Since δ_s in Hyb₁ experiment are computed by h , which are generated by PRF. Thus, any PPT \mathcal{A} cannot distinguish δ_s and $\tilde{\delta}_s$, given the security of PRF. If \mathcal{A} has the non-negligible advantage to guess the real s , then the \mathcal{A} can distinguish $\tilde{\delta}_s$ and δ_s with non-negligible probability, which breaks PRF.

$\Rightarrow \text{Hyb}_2 \equiv \text{Hyb}_1$.

Hyb₃: It is identical to $\text{Ideal}_{\mathcal{S}, \mathcal{F}}^{1^\lambda, \mathcal{A}}$, i.e., all the $\text{view}_0, \text{view}_1$ are simulated by $\mathcal{S}_0, \mathcal{S}_1$. The randomness of $b, \langle u \rangle_0, \langle bu \rangle_0, \delta_s, \delta_{\langle x \rangle_0}, \delta_{\langle x \rangle_1}, \delta_x$ guarantees no non-negligible \mathcal{A} 's advantage of distinguishability to \mathcal{S}_0 's view. Similarly, the randomness of $\langle bu \rangle_1, \langle u \rangle_1, \delta_{\langle x \rangle_1}, \delta_s$ guarantees no non-negligible \mathcal{A} 's advantage of distinguishability to \mathcal{S}_1 's view. Now, \mathcal{P}_0 cannot obtain $\langle x \rangle_1$, while \mathcal{P}_1 cannot obtain $s, \langle x \rangle_0$ since $\{\mathcal{S}_i\}_{i \in \{0,1\}}$ cannot obtain $\{\mathcal{S}_{1-i}\}_{i \in \{0,1\}}$'s inputs using $\{\text{view}_i\}_{i \in \{0,1\}}$.

$\Rightarrow \text{Hyb}_3 \equiv \text{Hyb}_2$.

So, $\text{Real}_{\Pi_{\text{OSM}}}^{1^\lambda, \mathcal{A}} \equiv \text{Ideal}_{\mathcal{S}, \mathcal{F}}^{1^\lambda, \mathcal{A}}$ for any PPT semi-honest \mathcal{A} . \square

E.3 Security of $\Pi_{(\text{SM})^2}$

Correctness has been checked using theoretical foundation for sparse-matrix in Appendix B. Functionality 3 defines arbitrary-sparse matrix multiplication without decomposition.

THEOREM 8 (SECURITY OF $\Pi_{(\text{SM})^2}$). *Let A be a sparse matrix and X be any vector/matrix. The protocol $\Pi_{(\text{SM})^2}$ realizes the functionality $\mathcal{F}_{(\text{SM})^2}$ against static semi-honest adversaries.*

PROOF. The $\Pi_{(\text{SM})^2}$ protocol sequentially call the independent subroutines of 5 Π_{OP} , 2 Π_{OSM} , and 1 Π_{Mult} protocols that have been proved to be semi-honest secure. The sequential composition theorem [10] guarantees that security is closed under composition. So, $\Pi_{(\text{SM})^2}$ is semi-honest secure. \square

E.4 Security of VIRGOS

THEOREM 9. *VIRGOS securely realizes the functionality of GCN (Figure 1) against static semi-honest adversaries.*

PROOF. VIRGOS integrates the semi-honest protocols for all elementary operations like graph convolution and activation layers. To obtain the secure inference or training protocol, we can sequentially compose the relevant protocols. Correctness and security of private inference or training follow the integration of underlying sub-protocols. By the sequential composition theorem [10], VIRGOS is semi-honest secure. \square